SYNTHESIS AND ALIGNMENT OF GOLD NANORODS FOR OPTICAL APPLICATIONS

BY

BETHANY LOIS GRILLO

THESIS

Submitted in partial fulfillment of the requirements
for the degree of Master of Science in Materials Science and Engineering
in the Graduate College of the
University of Illinois at Urbana-Champaign, 2014

Urbana, Illinois

Advisor:

Professor Catherine J. Murphy

ABSTRACT

Gold nanorods are of great interest in many areas of science and technology due to their versatility and electro-optical properties. There are simple synthesis methods that allow for shape control and the ability to change the chemistry on the surface of the gold nanorods. One of the interesting properties of gold nanorods is their ability to locally enhance electromagnetic fields in the vicinity of the ends of the nanorods. This enhancement can be increased and additive when multiple gold nanorods are aligned and can be useful for sensing and plasmonic enhancement. This study of alignment and surface chemistry of gold nanorods is to help elucidate simplistic ways to create large arrays of patterned gold nanorods through shear and directed assembly.

ACKNOWLEDGEMENTS

First, I would like to thank my advisor, Professor Catherine Murphy for her help and support throughout this work. I would also like to thank all of the members of the Murphy research group who have helped me along the way through instructions, discussions, and collaborations.

I would like to acknowledge the guidance of Dr. Monica Allen, Dr. Brett Wenner, and Dr. Jeff Allen as well as thank them for the opportunity to work with them at the AFRL. It was a unique and fulfilling experience.

Thank you, also, to my friends and family for keeping me laughing and smiling throughout my entire education and especially to my husband, Anthony. There is no way I would have been able to get here without your help, patience, and support. A final thanks to our faithful friend, Pippa who always reminds me that there is nothing in life more exciting than getting to be with the ones that you care about.

TABLE OF CONTENTS

CHAPTER 1

INTRODUCTION TO GOLD NANORODS AND APPLICATIONS

1.1 Introduction

For centuries scientists and artists alike have been interested in nano-sized metal particles. Artisans were using these particles in glass to make vibrant colors for beautiful objects such as the Lycurgus cup and colored-glass windows. Michael Faraday was studying the synthesis and optical properties of gold colloids at the turn of the 19th century following the interests of scientists and philosophers from the 16th century [1]. Current science and technology take advantage of metal nanoparticles of many shapes and types for applications in bio-sensors [2-7], plasmonics [6, 8-12], imaging [6, 13, 14], photothermal therapy [5, 6, 15], surface-enhanced Raman scattering [6, 16-19], and enhanced fluorescence [16, 20-22] due to their unique electro-optical properties.

The optical properties of these particles are of great interest to past and present technology in large part due to the surface plasmons that can be formed when light is incident upon them. The surface plasmons are the oscillations of the conducting electrons of the metal nanoparticle surface. Of particular interest is the resonance state that can

occur at specific frequencies of light due to the electrons being excited in-phase. The resonance causes enhancement of the scattering cross section and localized enhancement of electric fields [3, 6, 8, 18, 23]. These enhancements are greatest when the particles are much smaller than the wavelength of the incident light [6, 8, 23].

The wavelength at which the surface plasmon resonance occurs depends on the size, shape, and material of the nanoparticle as well as the refractive index of the medium in which the nanoparticles are dispersed [1, 8, 24]. Gold nanorods, specifically, have two distinct surface plasmon resonances (SPRs) in the UV and visible range of the electromagnetic spectrum that are easily tunable with slight variations in synthesis. There is one resonance that is due to the width of the nanorod, called the transverse SPR, and one caused by the length of the nanorod, called the longitudinal surface plasmon resonance (LSPR) [24]. An example of how both SPRs appear in UV-Visible spectra is shown in Figure 1.1. A red-shift of the LSPR occurs when the aspect ratio of the gold nanorods are increased while the transverse SPR remains at the same wavelength as shown in Figure 1.2 [25]. Size, aggregation, and changes in the media surrounding the gold nanorods can also be observed using UV-Visible spectrophotometry. At the LSPR wavelength the electric field intensity and absorption cross-sections are most strongly enhanced. Figure 1.3 shows TEM micrographs and corresponding UV-Visible spectra of gold nanorods of various aspect ratios.

The surface plasmons greatly enhance electromagnetic fields in the direct vicinity of the metal nanoparticles making them useful for waveguides and sensing devices. When multiple metal nanoparticles are aligned, the electric field enhancement increases

and the SPR peaks narrow [8, 10, 18, 21, 26]. This narrowing results in increased sensitivity. The spacing between the ends of the nanoparticles and varying the distances and angles between the particles will change the way in which light interacts with the system [10, 18, 21, 27-29]. The narrowest and most intense SPRs can be seen in arrays of nanoparticles with gaps of about 0.5 nm aligned end-to-end [30]. Varying the angle between nanoparticles will change the amount of electromagnetic radiation absorbed by the system with the peak absorbance occurring when light is polarized in the same direction as the alignment [8, 10, 27, 30].

Traditionally, the approaches for creating devices with patterned gold nanorods leave them with a set configuration. Using top-down methods such as electron-beam lithography [8, 31] or nanoimprinting can create homogeneous arrays, but it would be beneficial to have the ability to dynamically change the spatial orientation of the gold nanoparticles and do so in three dimensions.

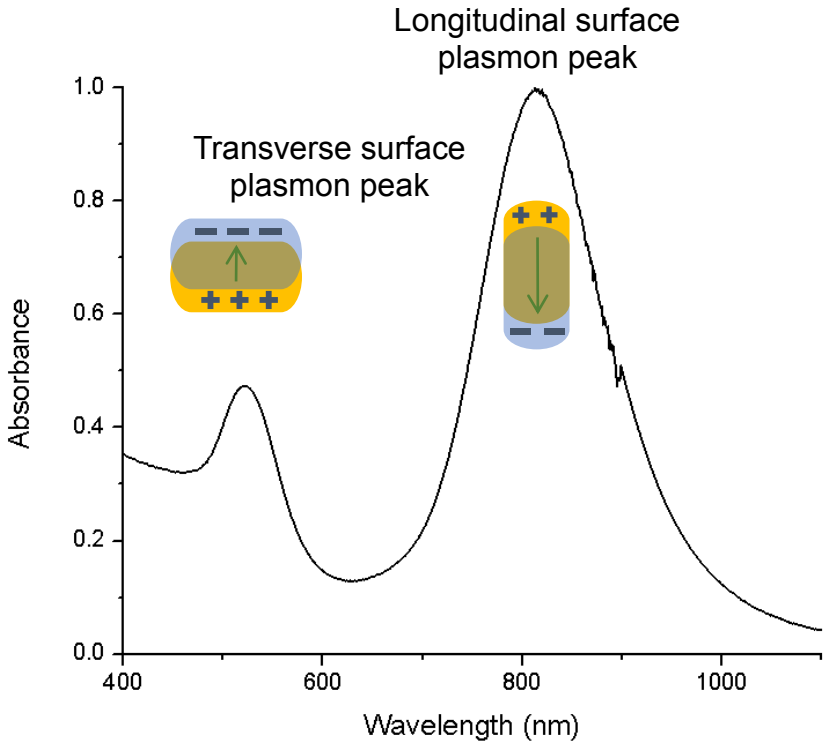

Figure 1.1 Example of gold nanorod UV-Vis spectra with diagrams describing the electron oscillations along the two axes within the nanorods.

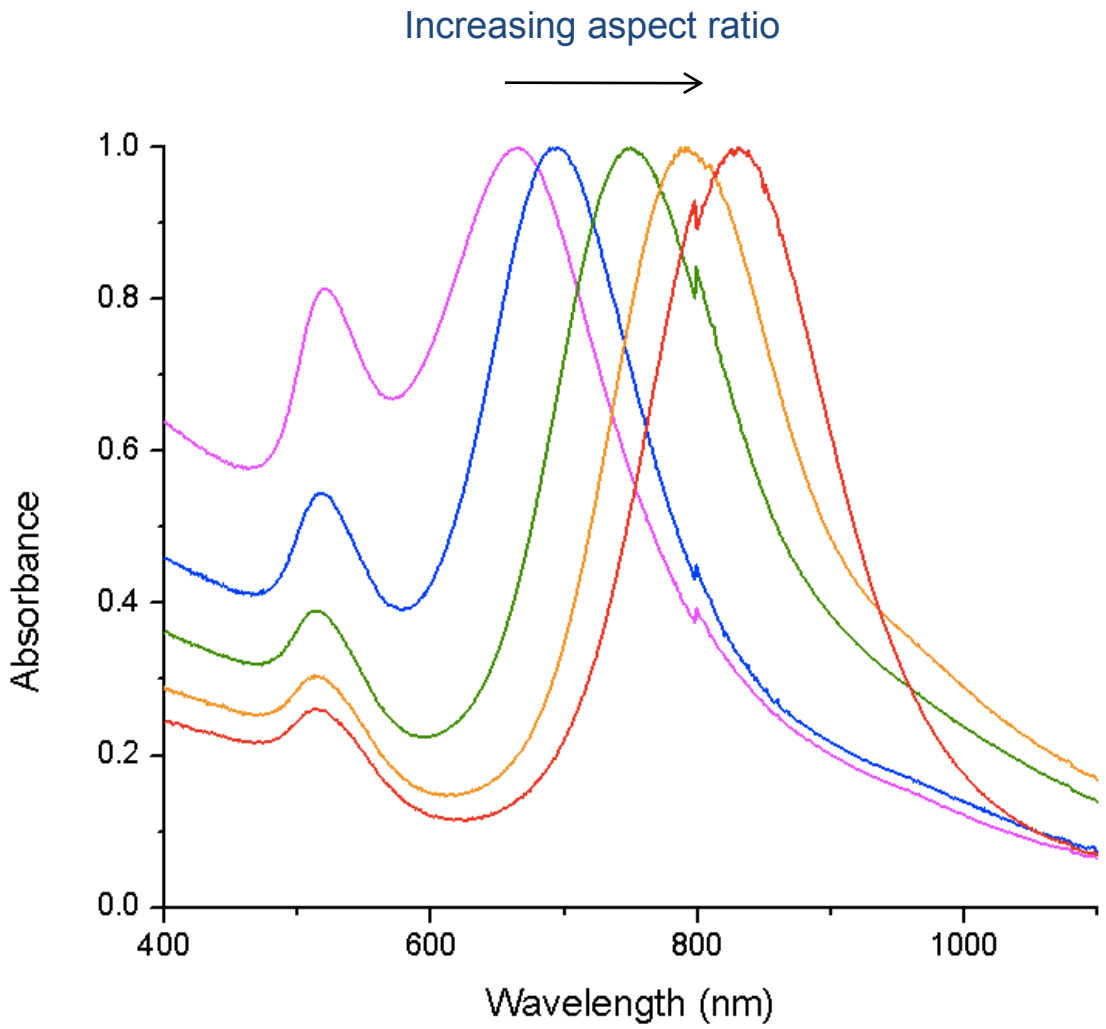

Figure 1.2 Normalized UV-Vis absorbance spectra of gold nanorods made with the standard synthesis and at various aspect ratios. The aspect ratio was varied by changing the amount of $AgNO_3$ added. The transverse SPR stays stationary around 525 nm and the LSPR wavelength changes from 664 nm up to 837 nm.

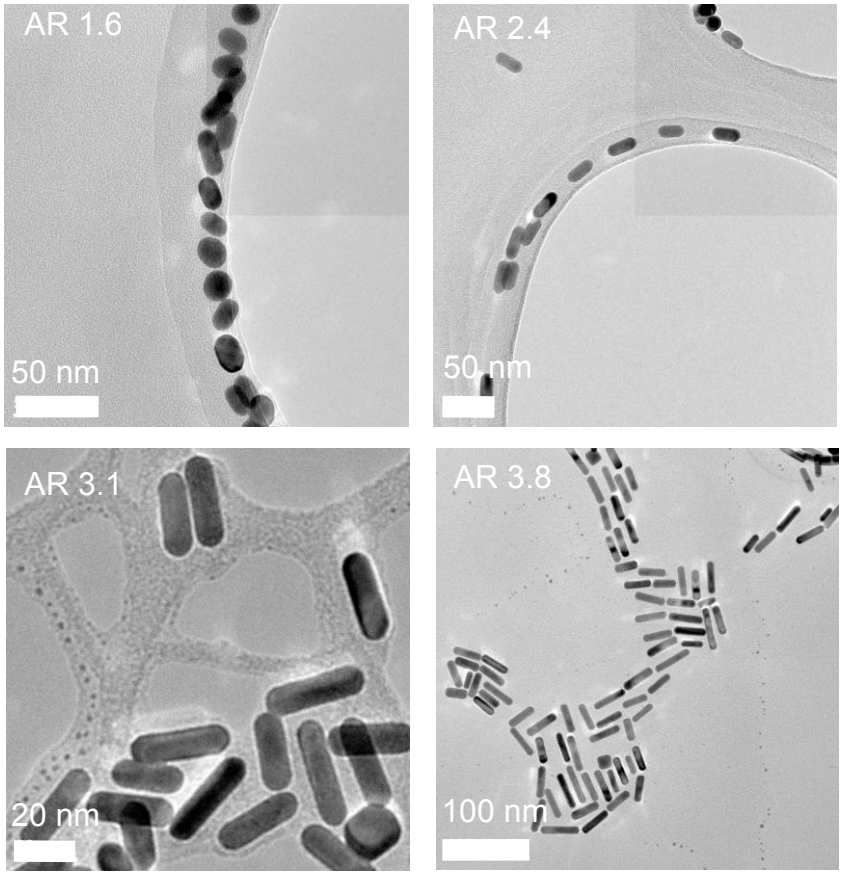

Figure 1.3 TEM micrographs of gold nanorods of different aspect ratios.

1.2 References

[1] El-Sayed, M. A. “Some Interesting Properties of Metals Confined in Time and Nanometer Space of Different Shapes” *Accounts of Chemical Research* **2001**, *34*, 257-264.

[2] Elghanian, R., J. J. Storhoff, R. C. Mucic, R. L. Letsinger, and C. A. Mirkin “Selective Colorimetric Detection of Polynucleotides Based on the Distance-Dependent Optical Properties of Gold Nanoparticles” *Science* **1997**, *277*, 1078-1081.

[3] Haes, A. J., R. P. Van Duyne “A Nanoscale Optical Biosensor: Sensitivity and Selectivity of an Approach on the Localized Surface Plasmon Resonance Spectroscopy of Triangular Silver Nanoparticles” *Journal of the American Chemical Society* **2002**, *124*, 10596-10604.

[4] El-Sayed, I. H., X. Huang, M. A. El-Sayed “Surface Plasmon Resonance Scattering and Absorption of anti-EGFR Antibody Conjugated Gold Nanoparticles in Cancer Diagnostics: Applications in Oral Cancer” *Nano Letters* **2005**, *5*, 829-834.

[5] Huang, X., I. H. El-Sayed, W. Qian, M. A. El-Sayed “Cancer Cell Imaging and Photothermal Therapy in the Near-Infrared Region by Using Gold Nanorods” *Journal of the American Chemical Society* **2006**, *125*, 2115-2120.

[6] Jain, P. K., X. Huang, I. H. El-Sayed, and M. A. El-Sayed “Noble Metals on the Nanoscale: Optical and Photothermal Properties and Some Applications in Imaging, Sensing, Biology, and Medicine” *Accounts of Chemical Research* **2008**, *41* 1578-1586.

[7] Sudeep, P. K., S. T. S. Joseph, K. G. Thomas “Selective Detection of Cysteine and Glutathione Using Gold Nanorods” *Journal of the American Chemical Society* **2005**, *127*, 6516-6517.

[8] Maier, S. A., M. L. Brongersma, P. G. Kik, S. Meltzer, A. A. G. Requicha, and H. A. Atwater “Plasmonics–A Route to Nanoscale Optical Devices” *Advanced Materials* **2001**, *13*, 1501-1505.

[9] Dickson, R. M., L. A. Lyon “Unidirectional Propagation in Metallic Nanowires” *Journal of Physical Chemistry B* **2000**, *104*, 6095-6098.

[10] Funston, A. M., C. Novo, T. J. Davis, P. Mulvaney “Plasmon Coupling of Gold Nanorods at Short Distances and in Different Geometries” *Nano Letters* **2009**, *9*, 1651-1658.

[11] Reinhard, B. M., S. Sheikholeslami, A. Mastroianni, A. P. Alivisatios, J. Liphardt "Use of Plasmon Coupling to Reveal the Dynamics of DNA Bending and Cleavage by Single EcoRV Restriction Enzymes" *Proceedings of the National Academy of Sciences* **2007**, *104*, 2667-2672.

[12] Sonnichsen, C., B. M. Reinhard, J. Liphardt, A. P. Alivisatos "A Molecular Ruler Based on Plasmon Coupling of Single Gold and Silver Nanoparticles" *Nature Biotechnology* **2005**, *23*, 741-745.

[13] Sonnichsen, C., A. P. Alivisatos "Gold Nanorods as Novel Nanobelaching Plasmon-Based Orientation Sensors for Polarized Single-Particle Microscopy" *Nano Letters* **2005**, *5*, 301-304.

[14] Sokolov, K., M. Follen, J. Aaron, I. Pavlova, A. Malpica, R. Lotan, and R. Richards-Kortum "Real-Time Vital Optical Imaging of Precancer Using Anti-Epidermal Growth Factor Receptor Antibodies Conjugated to Gold Nanoparticles" *Cancer Research* **2003**, *63*, 1999-2004.

[15] O'Neal, D. P., L. R. Hirsch, N. J. Halas, J. D. Payne, and J. L. West "Photo-Thermal Tumor Ablation in Mice Using Near Infrared-Absorbing Nanoparticles" *Cancer Letters* **2004**, *208*, 171-176.

[16] Emory, S. R., S. Nie "Near-Field Surface-Enhanced Raman Spectroscopy on Single Silver Nanoparticles" *Analytical Chemistry* **1997**, *69*, 2631-2635.

[17] Feldij, N., J. Aubard, G. Levi, J. R. Krenn, Salerno, G. Schider, B. Lamprecht, A. Leitner, F. R. Aussenegg "Controlling the optical Resonance of regular arrays of gold particles for surface-enhanced Raman scattering" *Physical Review B* **2002**, *65*, 075419.

[18] Kumar, J., K. G. Thomas "Surface-Enhanced Raman Spectroscopy: Investigations at the Nanorod Edges and Dimer Junctions" *Journal of Physical Chemistry Letters* **2011**, *2*, 610-615.

[19] Nie, S., S. R. Emory "Probing Single Molecules and Single Nanoparticles by Surface-Enhanced Raman Scattering" *Science* **1997**, *275*, 1102-1106.

[20] Eustis, S., M. El-Sayed "Aspect Ratio Dependence of the Enhanced Fluorescence Intensity of Gold Nanorods: Experimental and Simulation Study" *Journal of Physical Chemistry B* **2005**, *109*, 16350-16356.

[21] Huang, F., J. J. Baumberg "Actively Tuned Plasmons on Elastomerically Driven Au Nanoparticle Dimers" *Nano Letters* **2010**, *10*, 1787-1792.

[22] Mohamed, M. B., V. Volkov, S. Link, M. A. El-Sayed “The 'Lightning' Gold Nanorods: Fluorescence Enhancement of Over a Million Compared to the Gold Metal” *Chemical Physics Letters* **2000**, *317*, 517-523.

[23] Link, S., M. A. El-Sayed “Spectral Properties and Relaxation Dynamics of Surface Plasmon Electronic Oscillations in Gold and Silver Nanodots and Nanorods*” Journal of Physical Chemistry B* **1999**, *103*, 8410-8426.

[24] Haynes, C. L., A. D. McFarland, L. Zhao, R. P. Van Duyne, G. C. Schatz, L. Gunnarsson, J. Prikulis, B. Kasemo, M. Kall “Nanoparticle Optics: The Importance of Radiative Dipole Coupling in Two-Dimensional Nanoparticle Arrays” *Journal of Physical Chemistry B* **2003**, *107*, 7337-7342.

[25] Joseph, S. T. S., B. I. Ipe, P. Pramod, K. G. Thomas “Gold Nanorods to Nanochains: Mechanistic Investigations on Their Longitudinal Assembly Using α,ω-Alkanedithiols Interplasmon Coupling” *Journal of Physical Chemsitry B* **2006**, *110*, 150-157.

[26] Funston, A. M., T. J. Davis, C. Novo, P. Mulvaney “Coupling modes of gold trimer superstructures” *Philosophical Transactions of the Royal Society A* **2011**, *369*, 3472-3482.

[27] Shao, L, K. C. Woo, H. Chen, Z. Jin, J. Want, H.-Q. Lin “Angle- and Energy-Resolved Plasmon Coupling in Gold Nanorod Dimers” *ACS Nano* **2010**, *4*, 3053-3062.

[28] Barrow, S. J., A. M. Funston, D. E. Gomez, T. J. Davis, P. Mulvaney “Surface Plasmon Resonances in Strongly Coupled Gold Nanosphere Chains from Monomer to Hexamer” *Nano Letters* **2011**, *11*, 4180-4187.

[29] Rechberger, W., A. Hohenau, A. Leitner, J. R. Krenn, B. Lamprecht, F. R. Aussenegg “Optical Properties of Two Interacting Gold Nanoparticles” *Optics Communications* **2003**, *220*, 137-141.

[30] Kumar, J., X. Wei, S. Barrow, A. M. Funston, K. G. Thomas, P. Mulvaney ”Surface Plasmon Coupling in End-to-End Linked Gold Nanorod Dimers and Trimers” *Physical Chemistry Chemical Physics* **2013**, *15*, 4258-4264.

[31] Haynes, C. L., R. P. Van Duyne “Nanosphere Lithography: A Versatile Nanofabrication Tool for Studies of Size-Dependent Nanoparticle Optics” *Journal of Physical Chemistry B* **2001**, *105*, 5599-5611.

CHAPTER 2

SYNTHESIS OF GOLD NANORODS

2.1 Materials

Silver nitrate, hydroquinone, trisodium citrate, and Sodium borohydride ≥ 99 % were obtained from Sigma-Aldrich and used as received. Gold (III) chloride trihydrate, also known as chloroauric acid, ≥ 99.9 % was obtained from Aldrich and used as received. L-(+)ascorbic acid was obtained from Acros Organics and used as received. Sodium hydroxide was obtained from FisherChemicals and used as received. Hexadecyltrimethylammonium bromide (CTAB) (BioUltra, ≥ 99.0 %) and benzyldimethylhexadecylammonium chloride were obtained from Sigma and used as received. All of the glassware used in the following syntheses was cleaned prior to use with aqua regia and deionized (DI) water (18 mΩ). Aqua regia is 1:3 by volume concentrated nitric acid to hydrochloric acid. The same deionized water is used throughout the syntheses as well.

2.2 Instrumentation

Absorption spectra were primarily obtained using a Varian Cary 500 Scan UV-Vis-NIR spectrophotometer unless otherwise indicated. Other UV-Visible spectroscopy was

performed using a Perkin Elmer Lambda 900 UV-Visible-NIR spectrophotometer and in these instances it will be noted. Transmission electron microscopy (TEM) was performed using a JEOL 2100 Cryo TEM at an accelerating voltage of 200 kV. Scanning electron microscopy (SEM) was performed using a Hitachi S4800 High Resolution SEM. Dark field microscopy was performed using a Zeiss Axio Observer.Z1. Zeta potential measurements were obtained using a Brookhaven ZetaPALS instrument. Centrifugation was done using a Thermo Scientific Sorvall Legend X1 Centrifuge.

2.3 Standard Synthesis

It is only recently that scientists have been able to control the synthesis of gold nanorods, allowing the optical properties and size-dependence to be better understood. The first methods for synthesis used substrates of controlled pore size to electrochemically create anisotropic particles in the presence of CTAB [1]. This was followed by a simple three-step seeded growth method that creates gold nanorods with controllable aspect ratios between 18 and 25 that will be discussed in detail later [2, 3]. Since these initial methods were developed, variations have been shown to control different aspects of the final gold nanorod product.

The current standard procedure for creating gold nanorods of aspect ratios from approximately 2 to 5, which corresponds to lengths of 20 to 100 nm, is a seeded-growth method that produces gold nanorods in yields of greater than 95 % compared to other shapes and can be scaled-up to batches on the order of several liters [4]. The following

synthesis is modified from this method and describes the procedure used to make 10 mL batches and is used to create all of the gold nanorods hereafter described as being made using the standard synthesis.

First, a seed solution containing gold particles that are approximately 1.5 nm in diameter are made. A 0.1 M $HAuCl_4$ solution was made by adding 0.9846 g of $HAuCl_4$ to 25 mL of DI water with a Teflon-coated spatula and solution is then diluted by a factor of 10. This 0.01 M $HAuCl_4$ in the amount of 250 µL was reduced with 600 µL of freshly made, ice-cold 0.01 M sodium borohydride ($NaBH_4$) in a 9.75 mL aqueous solution of 0.1 M CTAB in a 50 mL centrifuge tube and stirring vigorously for 10 min after all additions have been made without capping. A 0.1 M $NaBH_4$ was made by adding 0.0430 g of $NaBH_4$ with a Teflon-coated spatula to 10 mL of DI water that had been cooled in an ice bath. 1 mL of this 0.1 M $NaBH_4$ solution is added to 9 mL of ice-cold DI water to create the final 0.01 M $NaBH_4$ solution. The aqueous CTAB solution is made by adding 36.4 g of CTAB to a 1 L volumetric flask, adding DI water to the 1 L mark, and stirring overnight.

A growth solution is made with 9.5 mL of 0.1 M CTAB to which $AgNO_3$ is added to achieve the desired aspect ratio of gold nanorods. With increasing amounts of $AgNO_3$ added, the gold nanorods will have increasing aspect ratios up to an aspect ratio of about 5. Spheres can be created in high yield using as little as 2 µL of 0.01 M $AgNO_3$ and the aspect ratio will increase with additions up to about 100 µL of 0.01 M $AgNO_3$. The 0.01 M $AgNO_3$ solution is made by adding 0.0169 g of $AgNO_3$ to 10 mL of DI water using a Teflon-coated spatula and being careful to keep the solution of $AgNO_3$ from light. Additions beyond this may actually decrease the aspect ratio of the gold nanorods for reasons that

have not been elucidated at this time. Figure 2.1 shows normalized UV-Vis absorbance spectra of gold nanorods made with various amounts of added $AgNO_3$ within the previously mentioned range. Figure 2.2 is an image of the “rainbow” of gold nanorods that can be created and shows that the aspect ratio of gold nanorods can be intuited from visual inspection. Table 2.1 shows the wavelength of the transverse SPR and LSPR of the absorbance spectra shown in Figure 2.1 by amount of $AgNO_3$ added.

After the $AgNO_3$ addition, 500 µL of 0.01 M $HAuCl_4$ is added creating an orange-yellow solution. Next, 55 µL of 0.1 M ascorbic acid (0.088g in 5 mL of DI water) is added and the solution is shaken vigorously until colorless. Lastly, 12 µL of the seed solution is added to the growth solution and left overnight before cleaning through two centrifugation cycles of 13,500 rcf for 20 min.

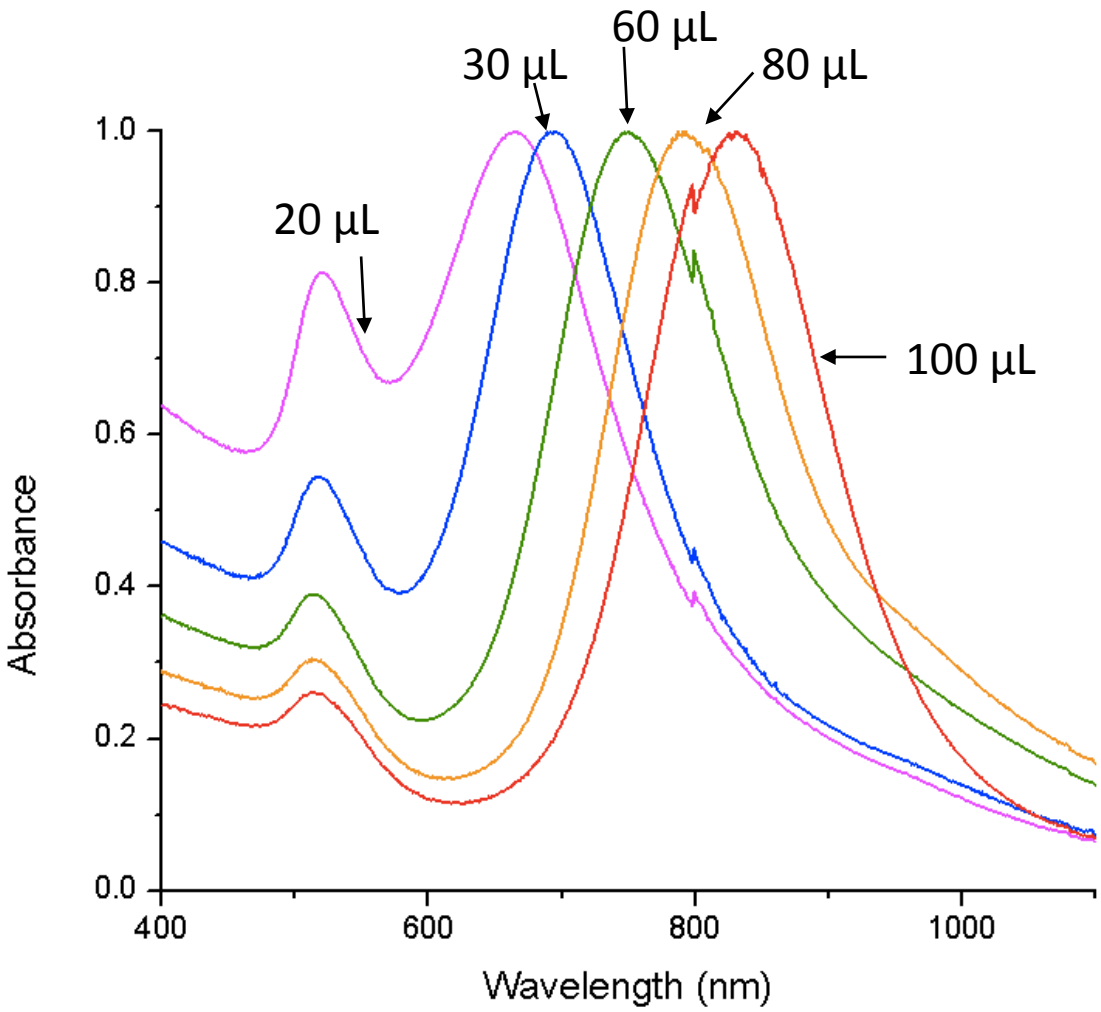

Figure 2.1 Normalized UV-Visible absorbance spectra of gold nanorods made with the standard synthesis and various amounts of $AgNO_3$ added. The amount of 0.01 M $AgNO_3$ added is denoted next to the spectra.

Figure 2.2 Picture of gold nanorods with aspect ratio increasing from left to right. The change in aspect ratio can be seen with the naked eye.

Table 2.1 Resonances of the longitudinal and transverse surface plasmons for various amounts of $AgNO_3$. These values correspond to the spectra showed in Figure 2.1.

Volume $AgNO_3$ added (µL)	**Transverse Surface Plasmon Resonance (nm)**	**Longitudinal Surface Plasmon Resonance (nm)**
20	528	664
30	524	700
60	525	777
80	523	808
100	523	837

2.4 Three-Step Growth Synthesis

Some applications require specific aspect ratios of gold nanorods that are larger than those produced by the standard synthesis above. To this end, another syntheses was attempted to gain the ability to reliably synthesize gold nanorods with LSPRs around 1064 nm as this double the wavelength of a 532 nm laser. Thus, a three-step growth method was attempted based on the synthesis by Busbee, Obare, and Murphy [2]. To begin, the seed solution was made and then allowed to sit for approximately 5 hours before proceeding. The seeds were made by adding 0.5 mL of 0.01 M $HAuCl_4$ and 0.5 mL of 0.01 M trisodium citrate (0.0294 g in 10 mL of DI water) to 19 mL of deionized water. Then, 0.6 mL of ice-cold $NaBH_4$ was added to the seed solution and stirred for 10 min.

Three growth solutions were prepared and labeled A, B, and C. Solutions A and B were each made in 15 mL centrifuge tubes and C is made in a 200 mL Erlenmeyer flask. Solutions A and B both contained 250 µL of 0.01 M $HAuCl_4$, 8.75 mL of 0.1 M CTAB, and 50 µL of 0.1 M ascorbic acid. Solution C is made up of 2.5 mL of 0.01 M $HAuCl_4$, 90 mL of 0.1 M CTAB, and 0.5 mL of 0.1 M ascorbic acid. All solutions were shaken and stirred until they were colorless.

To begin the growth 1 mL of seed solution was added to solution A. Solution A was then inverted to mix and 1 mL was added to solution B after 15 s. Solution B was then inverted to fully mix and the entirety of solution B was added to solution C after 30 s. The resulting solution was undisturbed for 14 h and then the entire contents of the flask was poured out and discarded. A few mL of deionized water was then used to recover the

desired long rods, with aspect ratios of approximately 20, from the bottom of the flask. This synthesis has a yield of approximately 90 % rods compared to other shapes [2, 3].

Gold nanorods with aspect ratios of 20 produce LSPRs at wavelengths much longer than 1064 nm. Shortening of growth times was attempted to produce gold nanorods with LSPR at shorter wavelengths, but were unsuccessful at doing such. Even after decreasing the time allowed for growth in each step the resulting gold nanorods of the three-step seeded growth method had aspect ratios that resulted in SPRs much larger than 1064 nm and, thus, not in range of the spectrophotometer. This meant that a new method was necessary, so the following co-surfactant method was attempted.

2.5 Co-Surfactant Synthesis

A method used in literature to push the LSPR of standard synthesis gold nanorods to higher wavelengths is a co-surfactant method. This method uses not only CTAB as a surfactant during synthesis, but also BDAC. Both are cationic surfactants with similar structures as shown in Figure 2.3. CTAB has a 16 carbon chain with a quaternary ammonium headgroup attached to three methyl groups and associated with a bromide ion as shown. BDAC is similar in that it is also made of a 16-membered carbon chain with a quaternary ammonium headgroup, but one of the attached groups is bulkier than a methyl group, C_6H_5, and the headgroup is associated with a chloride ion [5].

The aspect ratio of gold nanorods can be changed by varying the relative amounts of CTAB and BDAC so that the LSPR is changed from 900 up to 1300 nm. For

reproducibility and aiming for an LSPR of approximately 1064 nm the following procedure was chosen. Seeds were made by adding 0.6 mL of ice-cold 0.01 M $NaBH_4$ to 5 mL of 0.2 M CTAB and 5 mL of 0.0005 M $HAuCl_4$ (made by diluting the 0.01 M $HAuCl_4$ by 20) and then stirring vigorously for 2 min. The 0.2 M CTAB solution was made by adding 72.8 g of CTAB to a 1 L volumetric flask and then filling to 1 L with DI water before stirring for 15 to 20 min at 40 °C and then without heat overnight.

Two growth solutions were made, labeled A and B. Growth solution A started with 0.1 g of CTAB being added to 5 mL of an aqueous solution of 0.15 M BDAC (2.971 g BDAC in 50 mL of DI water) by heating to 40 °C while sonicating for 30 min. This was added to 200 µL of 0.004 M $AgNO_3$ (made by diluting 0.01 M $AgNO_3$ by a factor of 2.5 with DI water) and then 5 mL of 0.001 M $HAuCl_4$ (made by diluting 0.01 M $HAuCl_4$ by a factor of 100 with DI water). After gently mixing, 70 µL of 0.0788 M ascorbic acid was added followed by 12 µL of the seed solution. The 0.0788 M ascorbic acid was made by diluting the 0.1 M ascorbic acid by 1.27 times using DI water.

Growth solution B began with 0.1 g CTAB in 5 mL of 0.15 M BDAC added to 200 µL of 0.004 M $AgNO_3$ and then to 5 mL of 0.0005 M $HAuCl_4$. Ascorbic acid was the added in the amount of 36 µL with a concentration of 0.0788 M. Growth solution B was then slowly added to the growth solution A, that contained the gold seeds, at a rate of 1 mL every 20 minutes. After a simple test of varying numbers of additions of growth solution B to growth solution A it was determined that 6 additions would consistently produce gold nanorods with LSPR around 1064 nm, but with a yield of nearly 30-40 % spherical particles as evidenced by the UV-Vis in Figure 2.4. Although the paper that the original

synthesis was from reported yields of greater than 99 %, others also had yields closer to the results in Figure 2.4 [6, 7]. The UV-Vis results were confirmed by SEM of gold nanoparticles coated with poly(sodium-4-styrenesulfonate) (PSS) deposited on a surface of poly(allylamine hydrochloride) (PAH) done by the Heflin group at Virginia Tech. In literature, it has been shown that depletion of larger gold nanorods will occur with the additional surfactant. This allows for collection of these size-selected gold nanorods, but adds at least 24 h and many additional steps to the synthesis [6].

CTAB

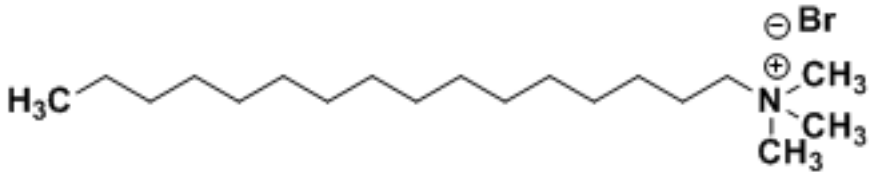

BDAC

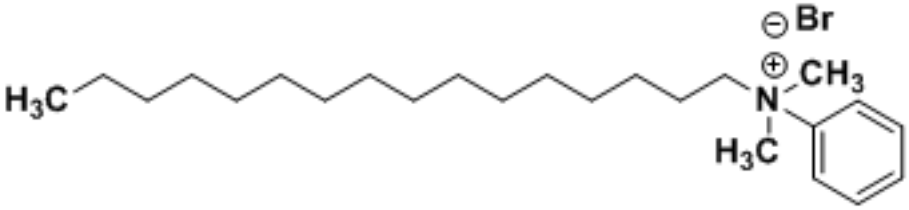

Figure 2.3 Structures of the two surfactants used in production of gold nanorods using the co-surfactant method.

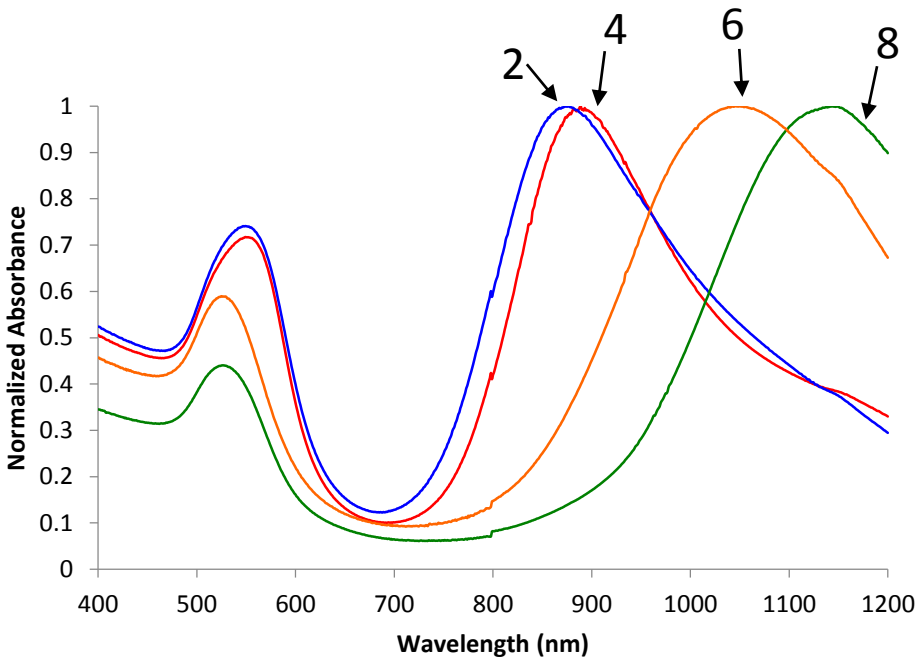

Figure 2.4 UV-Vis of BDAC/CTAB co-surfactant method synthesized gold nanorods. The transverse peak is large relative to the longitudinal peak indicating high concentrations of spheres. These traces indicate 2, 4, 6, and 8 additions of growth solution B to growth solution A and are labelled with the number of additions.

2.6 Hydroquinone Reduction Synthesis

As it seemed that the co-surfactant method produced far too many spherical particles a new method was attempted that changes the reducing agent used in the synthesis. The reducing agent is changed from ascorbic acid to the weaker reducing agent, hydroquinone. The formation of the gold nanorods slows down with the change, allowing for the longitudinal axis to grow longer while keeping the width nearly the same as that in the standard synthesis. The increased aspect ratio will push the LSPR to a higher wavelength. The yield is also improved using hydroquinone as the reducing agent [8].

This synthesis was similar to the standard synthesis described previously using ascorbic acid and is modified from the procedure given by Vidgerman and Zubarev [8]. First, seeds were made by using an aqueous solution of 5 mL 0.001 M $HAuCl_4$ and 5 mL of 0.2 M CTAB. The concentrations of $HAuCl_4$ and CTAB end up being the same as those in the standard synthesis, but the method was changed to more closely follow the synthesis described by Vidgerman and Zubarev. Next, 460 µL of 0.01 M $NaBH_4$ in 0.01 M NaOH was added to the seed solution. This $NaBH_4$ solution was used ice-cold and freshly made. A growth solution is made by adding 5 mL of 0.001 M $HAuCl_4$ and 5 mL of 0.2 M CTAB to 70 µL of 0.1 M $AgNO_3$ (0.169 g of $AgNO_3$ in 10 mL of DI water). Then, 500 µL 0.1 M aqueous hydroquinone (0.3441 g hydroquinone for 31.25 mL of DI water) was added to the growth solution. Finally, 160 µL of the seed solution was added to the growth solution. The solution then had a cloudy appearance and was left overnight before cleaning with two centrifugation cycles of 13,500 rcf for 20 min.

This synthesis proved to be the easiest and most reliable for producing high-yields of gold nanorods with LSPRs near 1064 nm. Figure 2.5 is a UV-Vis spectra shows the resulting gold nanorods varying the amount of added $AgNO_3$ from 40 µL to 80 µL and TEM micrographs are shown in Figure 2.6. Using TEMs, the over 400 particles were measured and found to have a width of 17 ± 2 nm, length of 97 ± 25 nm, and aspect ratio of about 5.8. Figure 2.7 shows TEM micrographs of gold nanorods made by the hydroquinone reduction synthesis compared to those made by the standard synthesis. The aspect ratio and longitudinal axis of the hydroquinone-reduced gold nanorods are obviously greater than those of the standard synthesis gold nanorods, but there also appears to be a difference in the shape of the gold nanorod ends. The ends of the hydroquinone-reduced gold nanorods appear to be less rounded than those in the standard synthesis and many of the sides appear to be more curved. These shape differences may change the way light interacts with the nanorods. The intermediate shapes that can be found in small numbers within the samples also seem to be more triangular and sharper vertexes. Both of these reasons could explain the differences between the transverse SPR peaks and the wavelengths lower than the LSPR from the two synthesis methods in the UV-Vis absorbance spectra shown in Figure 2.8.

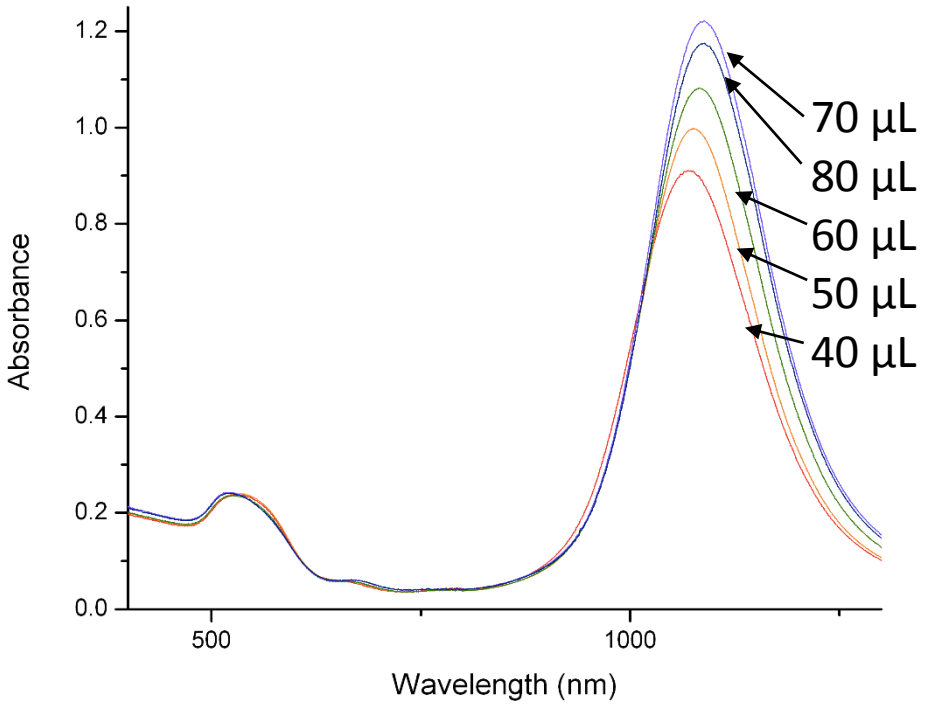

Figure 2.5. UV-Vis spectra of gold nanorods as-synthesized with the hydroquinone reduction method and with varying amounts of $AgNO_3$. Each trace is labelled with the volume of 0.1 M $AgNO_3$ that was added to the growth solution to create the gold nanorods.

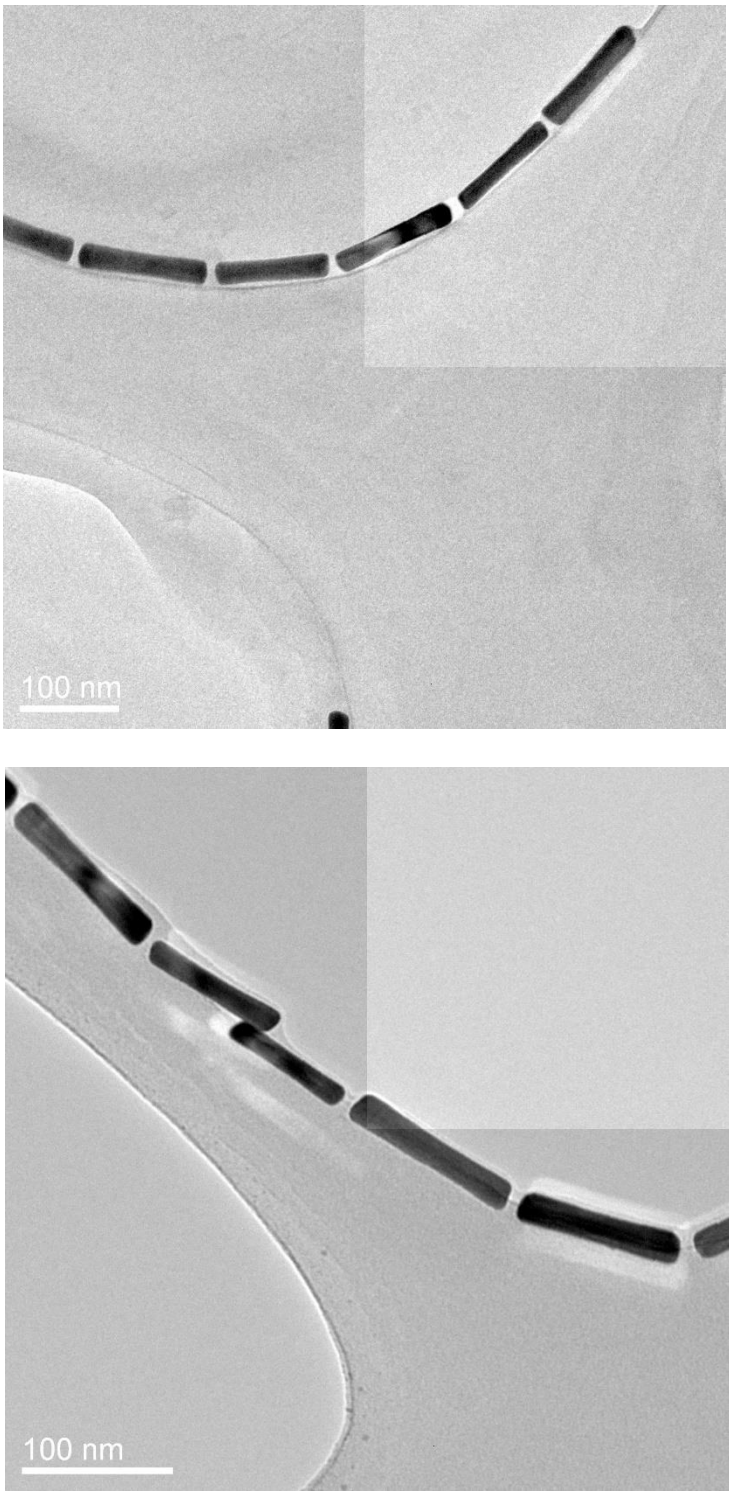

Figure 2.6 TEM micrographs of gold nanorods made with the hydroquinone reduction method.

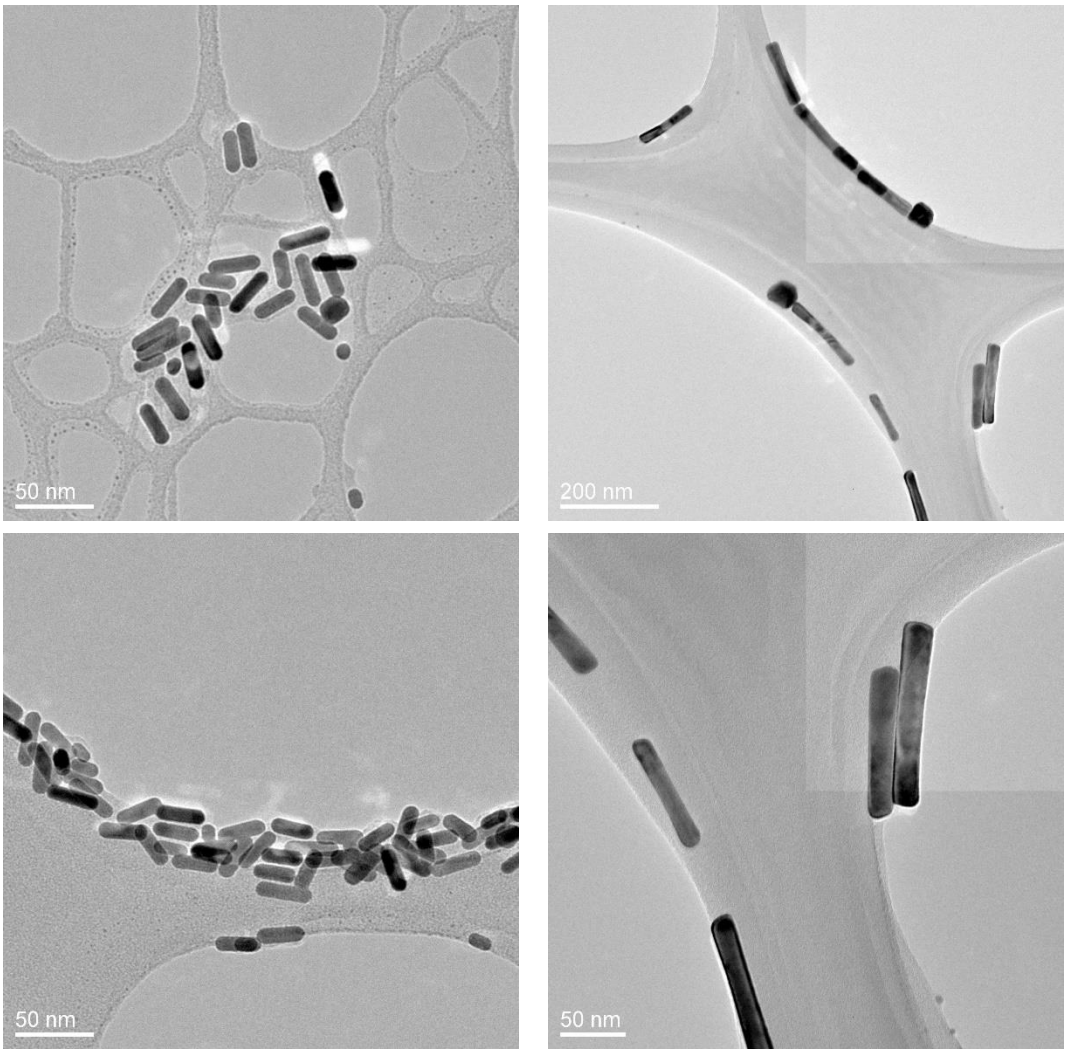

Figure 2.7 TEM micrographs of standard synthesis gold nanorods on the left compared to TEM micrographs of hydroquinone-reduced gold nanorods on the right.

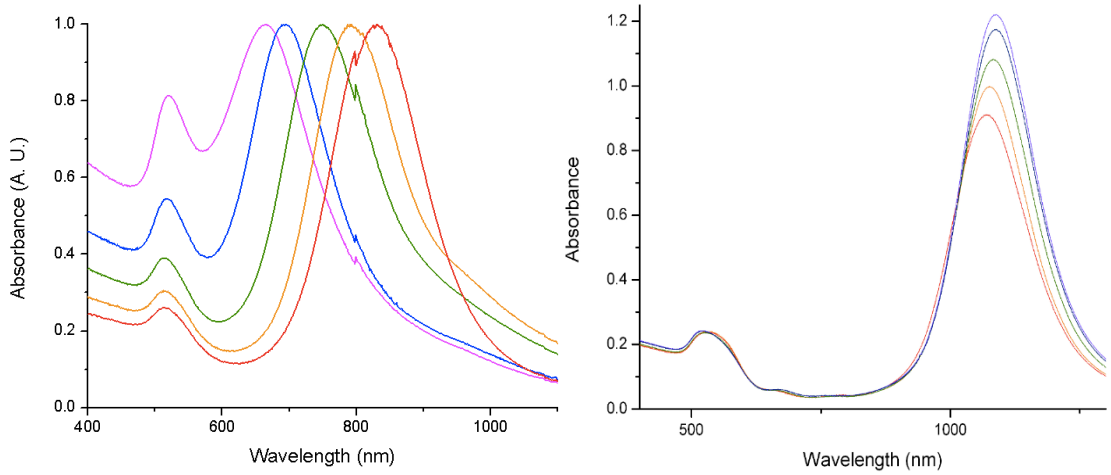

Figure 2.8 Side-by-side comparison of UV-Visible absorbance spectra from standard synthesis method (normalized, left) and the hydroquinone reduced synthesis (right). The shape of the spectra are different between about 500 nm and the beginning of the LSPR peak.

2.7 References

[1] Hulteen, J. C., C. R. Martin "A General Template-Based Method for the Preparation of Nanomaterials" *Journal of Materials Chemistry* **1997**, *7*, 1075-1087.

[2] Busbee, B. D., S. O. Obare, C. J. Murphy "An Improved Synthesis of High-Aspect-Ratio Gold Nanorods" *Advanced Materials*, **2003**, *15*, 414-416.

[3] Jana, N. R., L. Gearheart, C. J. Murphy "Wet Chemical Synthesis of High Aspect Ratio Cylindrical Gold Nanorods" *Journal of Physical Chemistry B* **2001**, *105*, 4065-4067.

[4] Sau, T. K., C. J. Murphy "Seeded High Yield Synthesis of Short Au Nanorods in Aqueous Solution" *Langmuir* **2004**, *20*, 6414-6420.

[5] Nikoobakht, B., M. A. El-Sayed "Preparation and Growth Mechanism of Gold Nanorods (NRs) Using Seed-Mediated Growth Method" *Chemistry of Materials* **2003**, *15*, 1957-1962.

[6] Liu, K., C. Resetco, E. Kumacheva "Salt-Mediated Kinetics of the Self-Assembly of Gold Nanorods End-Tethered with Polymer Ligands" *Nanoscale* **2012**, *4*, 6574-6580.

[7] Tsutusi, Y., T. Hayakawa, G. Kawamura, M. Nogami "Tuned Longitudinal Surface Plasmon Resonance and Third-Order Nonlinear Optical Properties of Gold Nanorods" *Nanotechnology* **2011**, *22*, 275203.

[8] Vidgerman, L., E. R. Zubarev "High-Yield Synthesis of Gold Nanorods with Longitudinal SPR Peak Greater than 1200 nm Using Hydroquinone as a Reducing Agent" *Chemistry of Materials* **2013**, *25*, 1450-1457.

CHAPTER 3

APPLICATIONS AND ALIGNMENT OF GOLD NANORODS

3.1 Polyelectrolyte Wrapping of Gold Nanorods

All of the synthesis methods described in Chapter 2 resulted in gold nanorods that are stabilized in solution by a cationic surfactant. In the case of CTAB, a bilayer is formed around the particle with the polar headgroups facing out towards the solution giving the gold nanorods an overall positive charge and hydrophilicity. While useful for some applications, the CTAB-coated gold nanorods are not ideal for use in biological applications (as CTAB is cytotoxic), devices that require gold nanorods to be in a non-polar solvent, or in polymer-nanoparticle composites with hydrophobic polymer matrices [1].

One of the simplest methods for changing the surface chemistry of gold nanorods has proven to be that of layer-by-layer wrapping of polyelectrolytes. When the gold nanorod surface is positively charged, a negatively charged polyelectrolyte will be electrostatically attracted to the surface, which in turn will attract positively charged polyelectrolytes. The process can be repeated many times to wrap a gold nanorod with

the desired thickness and surface chemistry [1]. This method for wrapping nanoparticles follows from work done in the past to coat surfaces with alternating polyelectrolytes [2-4]

For the following studies poly(allylamine hydrochloride) PAH $M_w \approx$ 15,000 g/mol, poly(sodium 4-styrene-sulfonate) (PSS) $M_w \approx$ 70,000 g/mol, and poly(acrylic acid) (PAA) $M_w \approx$ 15,000 g/mol (35 wt %) were obtained from Aldrich. Stock solutions of each polyelectrolyte must be made for use in the following procedures. A 10^{-2} M sodium chloride stock solution is made and then 1 mL of the stock solution is added to 9 mL of DI water. For PAH and PSS stock solutions, 100 mg is weighed out and put in the 10 mL of 10^{-3} M sodium chloride solution to give a final concentration of 10 mg/mL polyelectrolyte. For the PAA stock solution, 0.3 mL is added to the 10^{-3} M sodium chloride solution to give a final concentration of 10 mg/mL, as well. PAA is a weak anionic polyelectrolyte, PSS is a strong anionic polyelectrolyte, and PAH is a weak cationic polyelectrolyte. The molecular structure of the repeat unit for each polyelectrolyte is shown in Figure 3.1.

Polyelectrolyte layer-by-layer coating of gold nanorods began with CTAB-stabilized gold nanorods that had been cleaned once by a 13,500 rcf for 20 min centrifugation cycle. After the centrifugation step, the supernatant containing excess CTAB was removed and a gold nanorod pellet was left. Two pellets from 10 mL gold nanorod samples were combined in an unused centrifuge tube to double the concentration and a couple drops of DI water were added. To the pellets, 1 mL of 0.01 M NaCl and 200 µL of the desired 10 mg/mL polyelectrolyte stock solution were added simultaneously. The polyelectrolyte used in this step can be PAA or PSS as they are both

anionic and are electrostatically attracted to the cationic CTAB layer surrounding the gold nanorods. The molecular weight of the PSS, however, makes it more suitable for rods with large aspect ratios than those made with the CTAB short-rod synthesis. After the anionic polyelectrolyte addition, the gold nanorod solution was stirred and shaken for at least 30 min. The gold nanorods were then centrifuged again for 20 min at 13,500 rcf, removing the supernatant that contained excess polyelectrolyte. If a cationic surface was required, 1 mL of 0.01 M NaCl and 200 µL of PAH were added to the pellet and the process could continue by alternating anionic and cationic polyelectrolytes until the necessary coating had been realized making sure that the final step was the centrifugation and removal of the excess polyelectrolyte.

The efficacy of the coating can easily be characterized by shifts in UV-Visible spectra as well as zeta-potential measurements as the sign of the measurements will change after each successive coating [1]. Figure 3.2 shows UV-Visible spectra of three different aspect ratios of gold nanorods that were cleaned, wrapped with PAA, cleaned, and then wrapped with PAH. Figure 3.3 shows the zeta-potentials of the cleaned, CTAB, gold nanorods, PAA, and PAH-wrapped gold nanorods. The sign of the zeta-potential changes from slightly positive when only CTAB is on the surface, to highly negative when wrapped in PAA, and then highly positive when wrapped in PAH. The magnitude of the zeta-potential measurements indicate that the gold nanorods are stable in solution. If the excess polyelectrolyte is not thoroughly removed after centrifugation aggregation may occur and can be seen by a shoulder in the UV-Visible spectra on the right side of the LSPR peak as shown in Figure 3.4 and the magnitude of the zeta-potential will be smaller than about 15 or 20 mV.

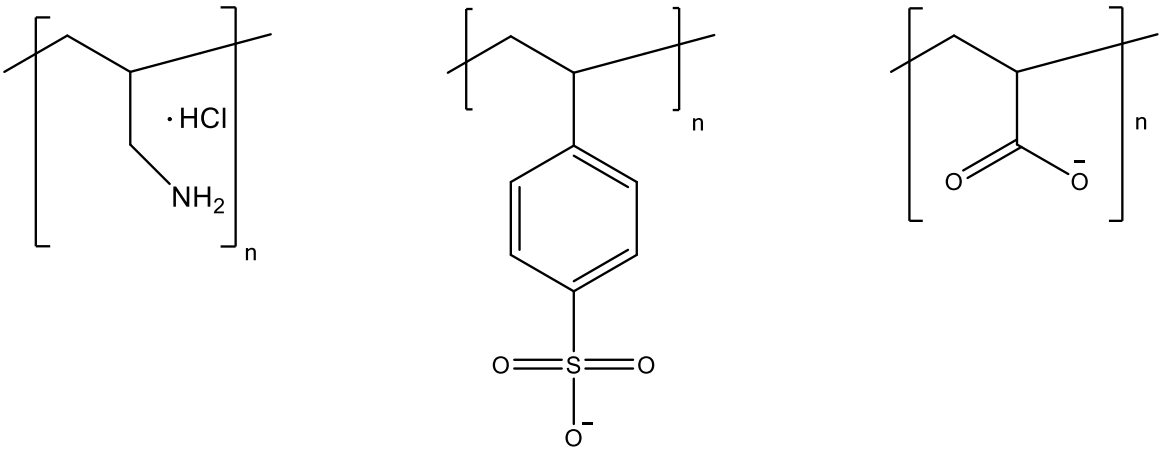

Figure 3.1. *Left*: Poly(allylamine hydrochloride) repeat unit molecular structure. *Middle*: Molecular structure of repeat unit of poly(sodium-4-styrenesulfonate). *Right*: poly(acrylic acid) repeat unit molecular structure.

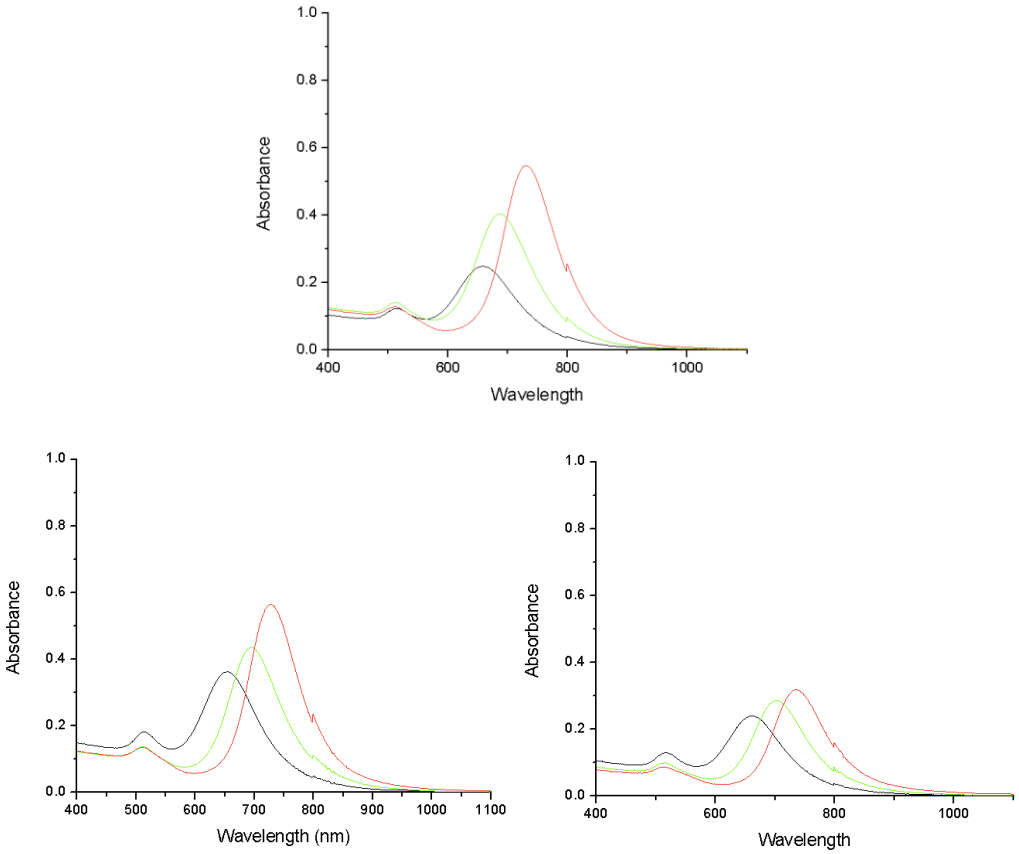

Figure 3.2 UV-Visible absorbance spectra of three different aspect ratios of gold nanorods before polyelectrolyte wrapping and after wrapping with PAA and then PAH. The dark lines that are the furthest left in each figure are of aspect ratio 2 gold nanorods, the green traces in the middle are aspect ratio 2.5, and the red trace on the right are gold nanorods with aspect ratios near five. The top figure is the cleaned CTAB-only gold nanorods. The figure on the bottom, left is after the gold nanorods have been wrapped in PAA. The figure on the bottom, right is after the gold nanorods have been wrapped in PAA and then PAH. The absorbance decreases with each sequential wrapping step because some gold nanorods are lost during centrifugation and cleaning steps.

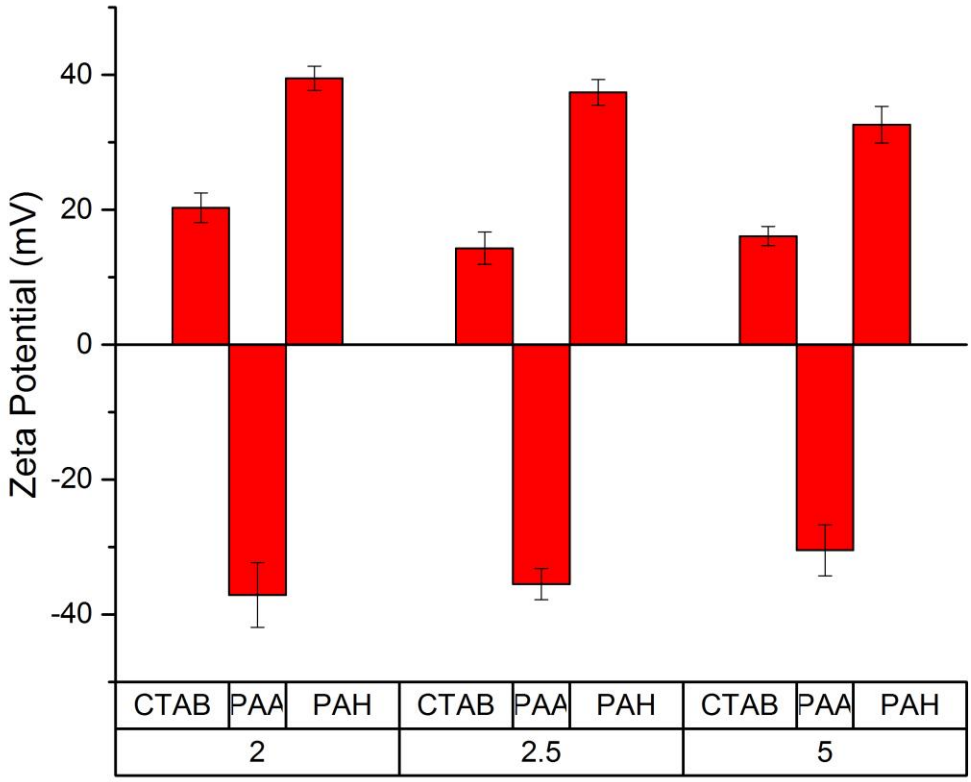

Figure 3.3 Zeta potential measurements of aspect ratio 2, 2.5, and 5 gold nanorods prior to wrapping, after wrapping with PAA, and after wrapping with PAH. The change in sign of the potential as well as the magnitude of the potentials indicate effective polyelectrolyte wrapping.

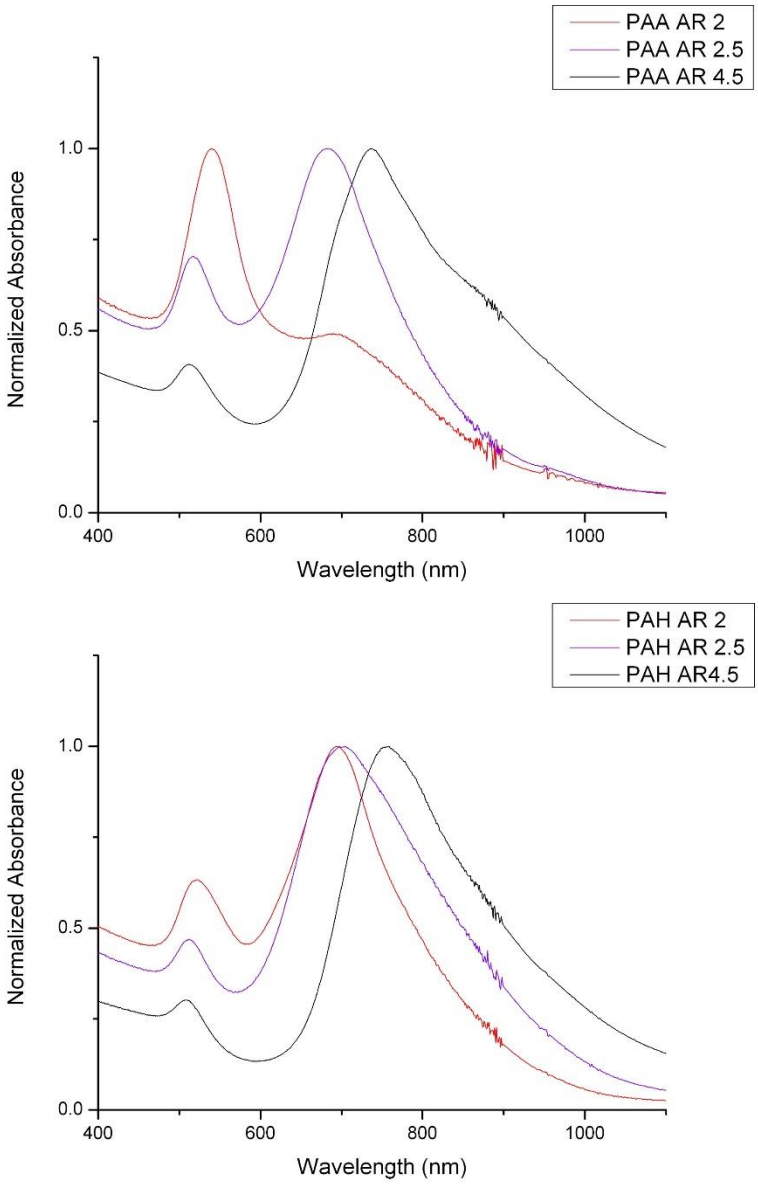

Figure 3.4 UV-Visible absorbance spectra of attempts at wrapping with PAA and PAH that aggregated. The aggregation can be inferred from the shoulders on the right side of the LSPR peaks.

3.2 Multilayer Structures for Field Alignment Experiments

Previous work has been done to align gold nanorods [5] and other nanoparticles [6- 8] in electric [5, 8] and magnetic fields [6, 7]. Some of this work has been in solution [5] and other with particles on a substrate [6- 8]. When depositing particles on a substrate they must be well-dispersed to allow for proper poling. This becomes an issue when gold nanorods in the aqueous phase are drop-cast onto a substrate. During the evaporation process gold nanorods tend to aggregate and form clumps so that they are not spread evenly upon the substrate.

To solve this issue, particles that have an opposite charge of the substrate surface can be used or the gold nanoparticles can be deposited within a polymer film. Simple chemical methods can be used to alter the charge of a substrate and polyelectrolyte-wrapping of gold nanorods can make them highly charged both positively and negatively as described previously. Polymer-nanoparticle films can be made with the two-step seeded-growth method nanoparticles that are CTAB-coated with polymers that are water-soluble.

Multilayer structures were produced by drop-casting of gold nanorods in polymer solutions onto 1 inch quartz substrates for testing the ability of poling using electric, magnetic, and electromagnetic fields. The quartz substrates were cleaned using an RCA method to leave the surface with a negative charge. To clean the substrates they are immersed in a 70 °C water, hydrogen peroxide, and ammonium hydroxide solution at a ratio of 6:2:1 for 20 min, rinsed in deionized water. Then, the substrates are immersed in a 70 °C solution of water, hydrogen peroxide, and hydrochloric acid at a ratio of 6:2:1 for

20 min, rinsed in deionized water once more, and finally dried for an hour at 130 °C. The desired first-layer was then drop-cast onto the surface in the amount of 0.5 mL and was left to dry overnight at room temperature. The specimen was then rinsed by placing it in a petri dish with DI water for 20 min and then dried at 60 °C for 30 min. A second layer was drop-cast on top of the first layer again using 0.5 mL. After an hour the specimen was wicked dry with a laboratory wipe and then placed in water for 30 min before drying at 60 °C for 30 min. These samples were then sent to the Air Force Research Labs for poling studies. SEM micrographs were taken to visualize the dispersion of the specimen and several are shown in Figure 3.5. Polyelectrolyte-wrapped gold nanorods of aspect ratios 2, 2.5, and 5 were used and placed in PAA or PAH solutions.

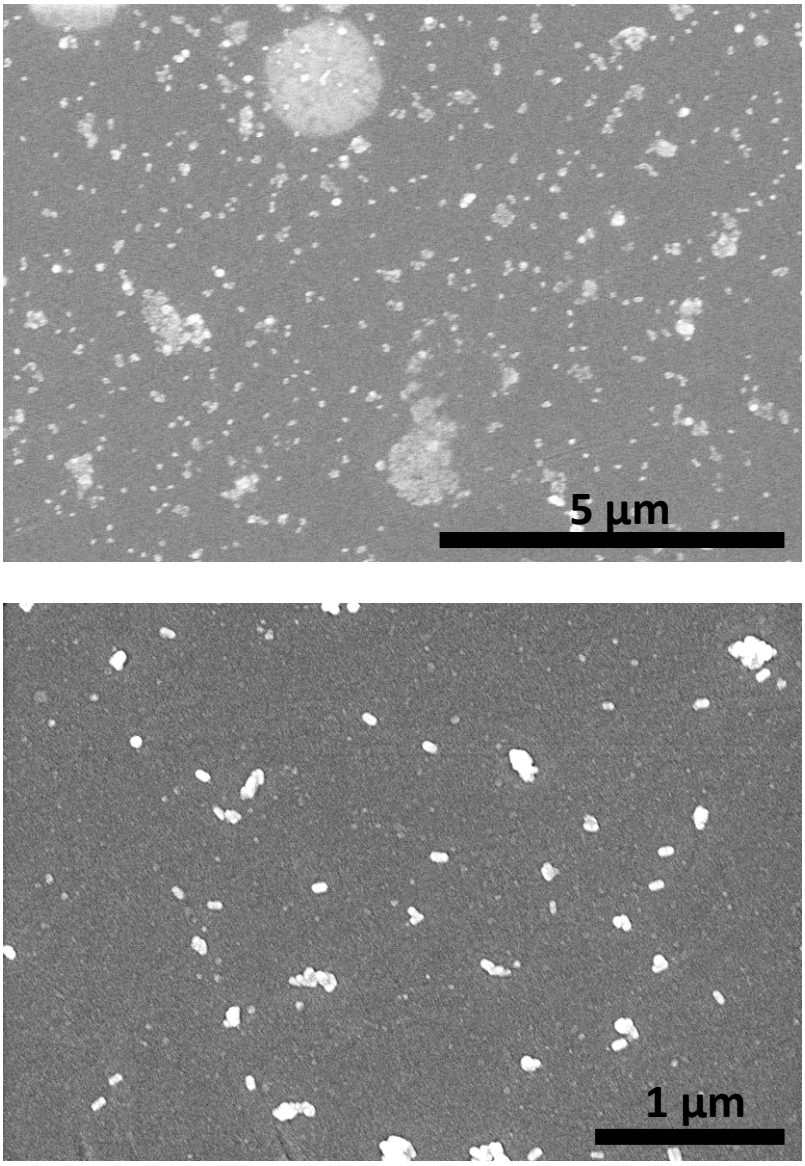

Figure 3.5 SEM micrographs of polyelectrolyte-wrapped gold nanorods in polymer films. *Top*: Aspect ratio 2, PAA-wrapped gold nanorods in PAH. *Bottom*: Aspect ratio 5, PAA-wrapped gold nanorods in PAA layered over PAA-wrapped, aspect ratio 5 gold nanorods in PAH.

3.3 Applications in Second Harmonic Generation

Second-order nonlinear optical (NLO) materials are used to make green and blue lasers, modulators, optical switches, and parametric amplifiers. Second harmonic generation (SHG) is one of these NLO processes that can be used for probing surfaces and interfaces. Second harmonic generation can occur when light from a laser of sufficient intensity impinges on a medium at a particular frequency. This light induces dipole oscillations of the molecules within the medium and the anharmonicity of the oscillations allows for the emission of electromagnetic radiation at not only the fundamental frequency, but also at harmonics such as those that are double or triple the fundamental frequency. The second harmonic that is emitted from the medium can be collected and used for spatial and temporal resolution of surfaces and has a wavelength that is half that of the impinging light [9].

Typically, NLO devices are made from inorganic crystals that require expensive and complicated production for crystals of desired size and quality. One method that has been attempted to overcome this issue is using ionic self-assembled monolayer (ISAM) films. ISAM films are essentially films with layers that alternate between polycation and polyanion created by immersing a substrate in alternating solutions of the polycations and polyanions using dyes in the layers for the NLO media [2, 10]. These ISAM films are created and studied by Heflin and group. To increase the effectiveness of these films, particles with SPRs can be used to enhance electromagnetic intensity locally as well as enhancing SHG [11-14]. Surface plasmons have proven to be beneficial in enhancing SHG [11, 15, 16]. In the past, silver triangle arrays were created using nanosphere

lithography to increase SHG conversion efficiency to good effect. These triangles, however, did not have regular spacing or geometry. To improve geometry irregularities gold nanorods were to be studied in place of the silver triangle arrays [11].

Gold nanorods with LSPR at approximately 1064 nm that could be deposited on a PAH-coated surface were needed. To this end, various methods of synthesizing gold nanorods were explored as described previously. The three-step method produces gold nanorods that have aspect ratios much too high for this LSPR. The standard short-rod synthesis could at best push the LSPR to about 920 nm, but there is still considerable absorbance at 1064 nm. The BDAC and CTAB co-surfactant method was unreliable and produced gold nanorods at almost the same yield as gold spheres. The spheres do not allow for the SHG to be enhanced as by the Heflin and Robinson groups at Virginia Tech. This leaves the hydroquinone reduction method as the best possible route for the synthesis and as such gold nanorods made using this method were used for SHG studies done by the Heflin and Robinson groups at Virginia Tech. Deposition on the ISAM films was attempted with PSS-wrapped gold nanorods as they have the opposite charge of the PAH films to which they will be exposed. However, these gold nanorods did not greatly increase SHG either. This is believed to be due in part to the distance between the particles and the film being too great for the near-field enhancement to occur. To this end, new surface chemistries will be explored in the future that allow for the plasmonic particles to be in closer contact with the NLO substrate.

3.4 Applications in Switchable Optical Materials

In the past, it has been shown that anisotropic nanoparticles can be aligned when embedded in a polymer film that has been stretched [17, 18]. Aligning gold nanorods gives even greater enhancement of optical properties due to near-field coupling [19- 21]. Methods for aligning nanoparticles previously included preferential end-to-end binding [21-24], block-copolymer templates [6], controlled evaporation [25], electric fields [5, 8, 26], magnetic fields [6, 7], and shear [17, 18]. In this study, shear was used to assemble the particles that are dispersed in a poly(vinyl alcohol) (PVA) matrix as it allows for simple reorientation and alignment by mechanical stretching. UV-Vis spectrophotometry shows the changes in optical properties that are caused by the mechanical stretching and using polarized light the anisotropic reorientation can be elucidated. This reorientation was compared to the alignment that could be achieved using the tracks of a digital versatile disc (DVD) as a template for similar polymer-nanoparticle composites.

Films were made in polystyrene 60 mm Petri dishes chosen for ease of film removal as well as capability of being heated to the necessary temperatures. A well-mixed solution containing 3 mL of 5 wt % poly(vinyl alcohol) (PVA) and 1 mL of aqueous gold nanorods at a chosen concentration is poured into the Petri dish. For this study the final concentration was chosen to be 1 nM. The PVA solution is made by adding 2.5 g of PVA (molecular weight 85-124k) purchased from Aldrich to 50 g of DI water and heated to 110 °C. The gold nanorods are added after allowing the PVA to cool. The dish was then put in a desiccator to remove air bubbles that have formed during mixing for 30 min. After this, the dish was placed in an oven set at 60 °C for 18 hr. The films were easily removed

and could be stretched up to four times their original size by hand if heated to at least 60 °C in a humid environment. Figure 3.6 shows that differences in gold nanorod concentration within the PVA films are visible to the naked eye.

These films allow for alignment from simple mechanical stretching, but the spacing is uneven and unpredictable due to the randomness of the process and drying effects. One way to attempt to overcome this flaw is to pattern the nanorods by directed-assembly. This was attempted through the use of a DVD as a mold for the film to be formed upon. DVDs contain grooves that are 320 nm wide and 740 nm apart center-to-center. When the film is dried onto this surface there will be enough room for the gold nanorods to be randomly oriented within the grooves and then align along the grooves when stretched. This creates an array of more uniformly-spaced gold nanoparticles that will allow for more repeatable results and increased efficiency of devices.

The grooves of a DVD are on the inner surfaces of two polycarbonate discs that are bonded together and can be accessed by cutting into the edge of a disc with scissors and then baking for about 1 min in an oven set at 80 °C. Both sides of the DVD can be used after removal of a metal film and organic dye. The metal film can be removed most easily using tape to pull it off and the organic dyes can be removed using isopropyl alcohol or methanol, depending on the brand of DVD. The two halves were then dried using flowing nitrogen and ready for the films to be poured and are shown in Figure 3.7. No alteration of the PVA and gold film solution is needed except that 4.5 mL of total solution is used as some can go under the DVD template and not be a part of the final film and it can be easily removed from the template as shown in Figure 3.8.

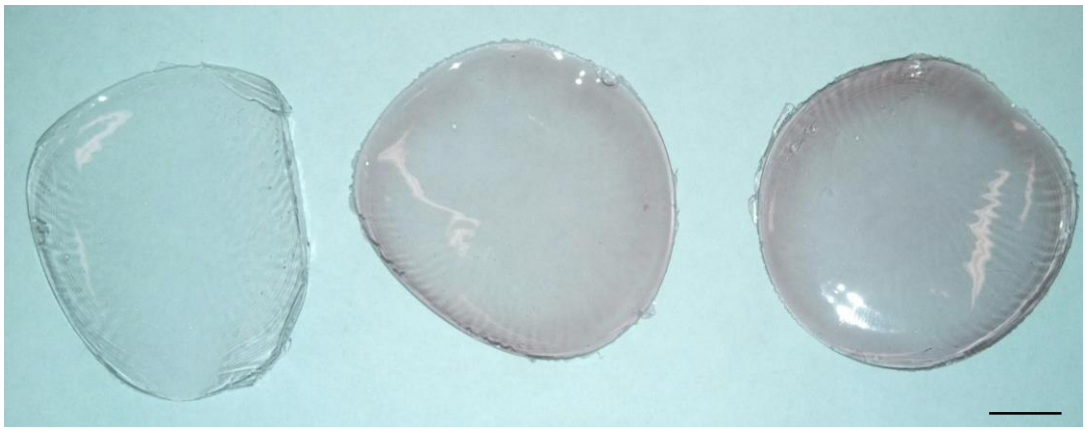

Figure 3.6 PVA films with concentrations increasing from left to right. Scale bar = 10 mm.

Figure 3.7 Image of DVD-R used to template polymer-nanoparticle composites. The image shows the two halves of the DVD-R after separation and prior to removal of dies and metallization layers.

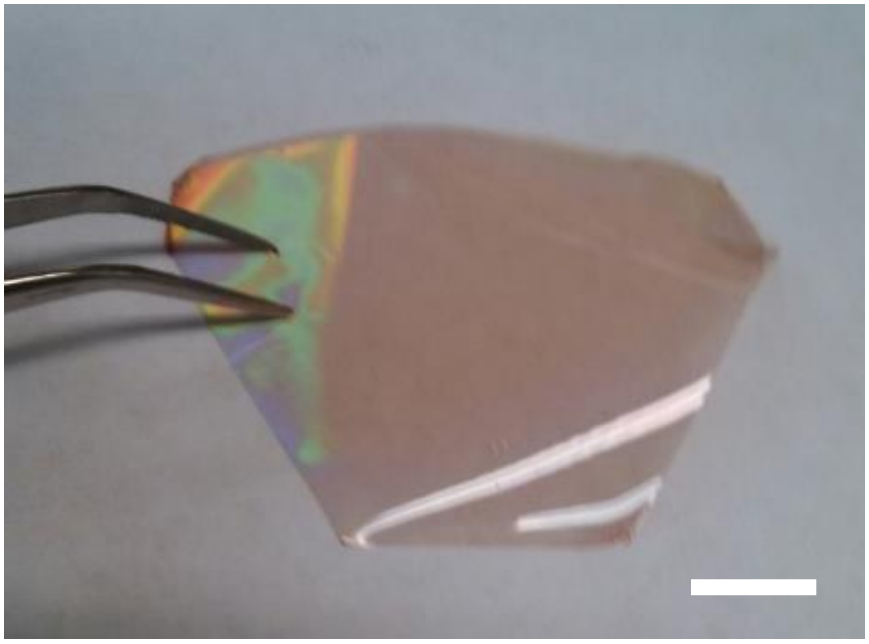

Figure 3.8 Image of polymer-nanoparticle composite film made on a DVD-R template. This film has been removed from the template and dish. The left side shows diffraction from the grating structure that has been transferred to the polymer-matrix. Scale bar is approximately 10 mm.

Three types of films were made to compare effectiveness of alignment using a template. The first type is untemplated nanoparticle-polymer films, the second is films that were templated using a DVD and then stretched along the tracks (referred to as parallel-stretching), and, lastly, films that were template using a DVD and stretched perpendicular to the tracks. SEMs of unstretched and stretched samples of are shown in Figure 3.9. The change in structure due to stretching is apparent in the SEMs of the templated samples. The parallel-stretched shows that the features from the grating-structure have become thinner and the perpendicular-stretched sample shows elimination of the grating-structure, but with some obvious directionality that is likely left over from the tracks.

The effect of orienting of nanorods preferentially along a specified axis can be verified using dark field microscopy, atomic force microcopy (AFM), and UV-visible absorbance spectra. Dark field microscopy can give qualitative evidence of alignment of gold nanorods. This is because they scatter light very strongly and in a polarized manner, meaning that alignment can be inferred by scattering when light is polarized in the same direction as the longitudinal axis of the rods [27]. The images in Figures 3.10 and 3.11 indicate that after stretching there appears to be increased scattering in many locations when the light is polarized along the direction that the films were stretched.

Another approach to determining efficacy of alignment is UV-Vis. Figure 3.12 shows the UV-Vis of the unstretched and stretched films that were made without templates in three different polarization states. Figure 3.13 shows the UV-Vis of templated samples that are unstretched, stretched along the track direction, and stretched perpendicular to the track direction. Figure 3.14 compares the three types of stretched

films in light that is polarized in the direction that the samples were stretched and, therefore, the longitudinal axis of the gold nanorods. In all of the unstretched films the polarization of the light does not change the absorbance as the gold nanorods are oriented randomly. After stretching, each type of sample shows near elimination of the LSPR peak in the spectra obtained using light polarized perpendicular to the stretch direction and spectra that were very similar in unpolarized light and light polarized along the stretch direction. This shows that few rods are unaligned after stretching and that the direction of alignment is such that the longitudinal axis of the gold nanorods follows the stretch direction. Comparing the spectra of the three types of film does not give a quantitative method of analyzing alignment as neither the film thickness nor the spacing of the gold nanorods can be controlled. The thickness of the PVA will change the background absorbance, so different films cannot be compared. If the spacing of the gold nanorods is not controlled the increased absorbance due to near-field enhancement is unknown. AFM of the samples can allow for qualitative determination of alignment, thickness of the PVA films, and spacing of the gold nanorods.

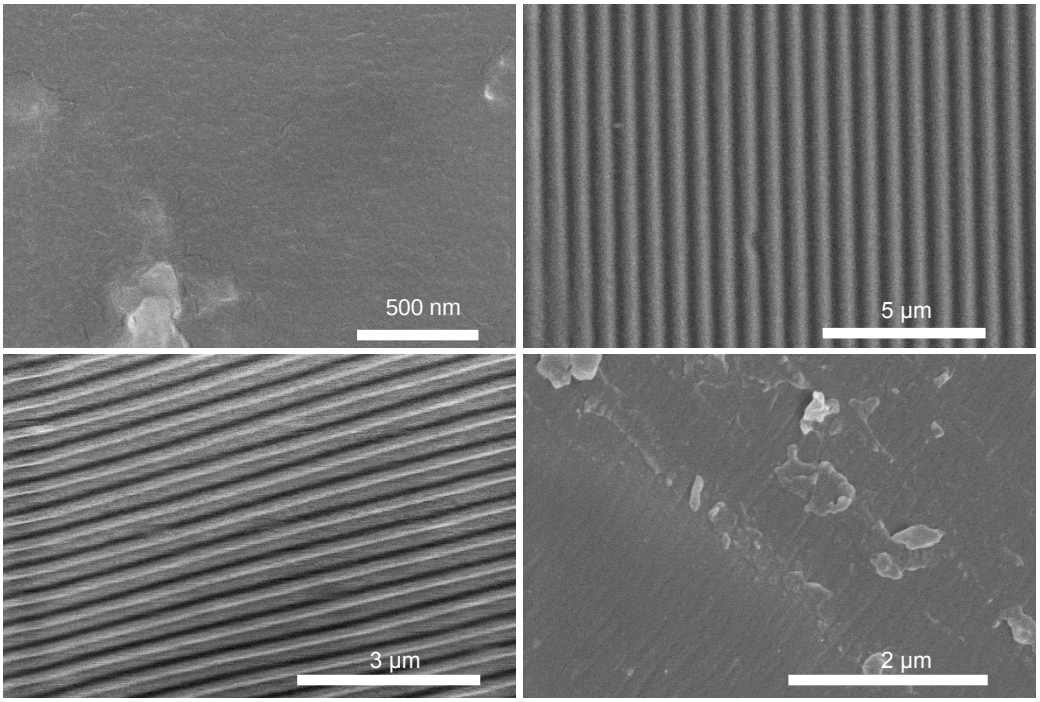

Figure 3.9 SEM micrographs of polymer-nanoparticle composite films: Made with no template and unstretched (top, left), made with DVD template and unstretched (top, right), made with DVD template and stretched along the track direction (bottom, left), and made with DVD template and stretched perpendicular to the track direction (bottom, right).

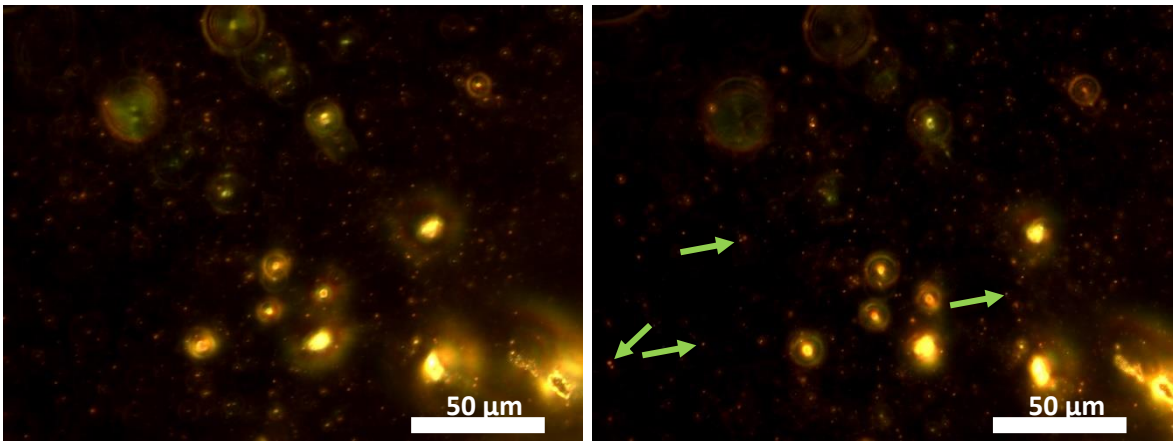

Figure 3.10 Dark field micrographs of polymer-nanoparticle composite films after stretching made with no template. The left was taken with polarization perpendicular to the stretch direction and the right with polarization parallel to the stretch direction. The green arrows point to several aligned gold nanorods that appear due to the polarization of the scattering.

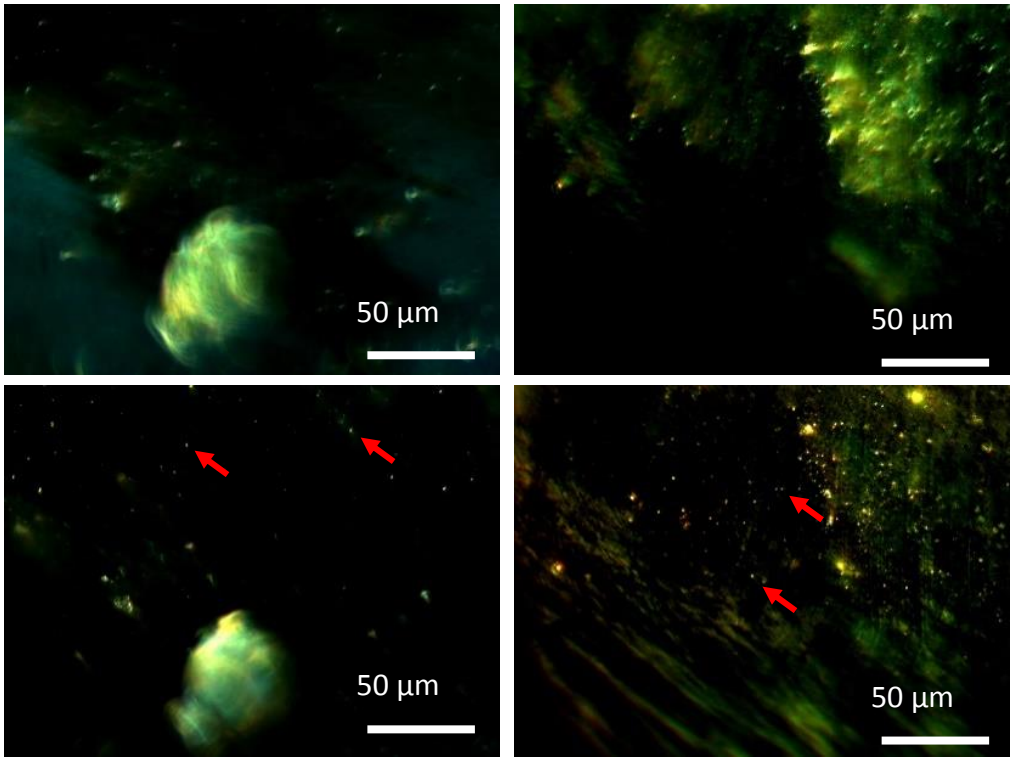

Figure 3.11 Dark field micrographs of polymer-nanoparticle composite films after stretching made with a DVD-R template. The micrographs on the left side are from the films stretched in the direction of the tracks and the micrographs on the right side are of the films stretched perpendicular to the track direction. The top row of micrographs were taken using only light polarized perpendicular to the stretch direction. The bottom row of micrographs were taken using light polarized along the stretch direction. The red arrows point to several of the scattering sites that are visible only in the micrographs of the light polarized in the direction of the longitudinal axes of the gold nanorods.

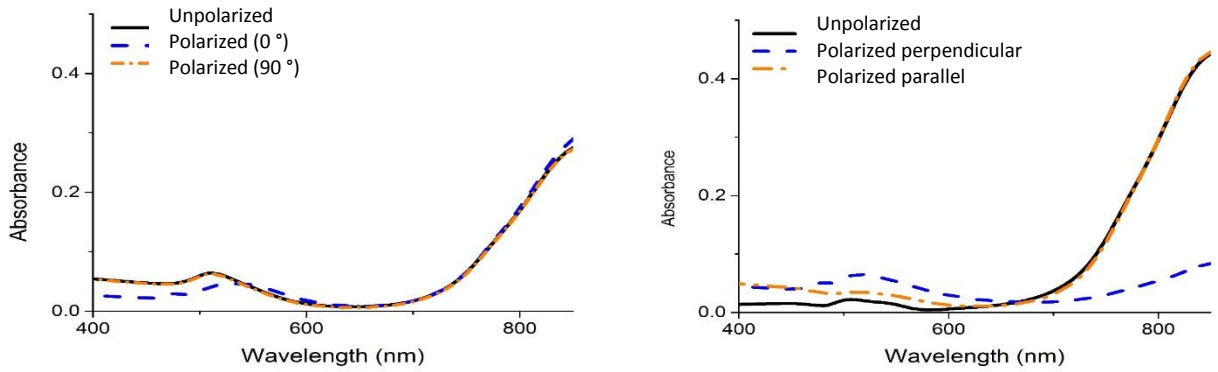

Figure 3.12 UV-Vis absorbance spectra of polymer-nanoparticle composite films before (left) and after (right) stretching. These were taken using the Perkin-Elmer Lambda 900 UV-Vis-NIR spectrophotometer. The solid black traces (———) are of spectra obtained in unpolarized light. The blue, dashed lines (- - -) are spectra obtained using light polarized perpendicular to the stretch direction for the stretched sample and 0° for the unstretched sample. The orange, dash-dot traces (- · -) are UV-Vis spectra obtained using light polarized along the stretch direction for the stretched sample and 90° for the unstretched sample.

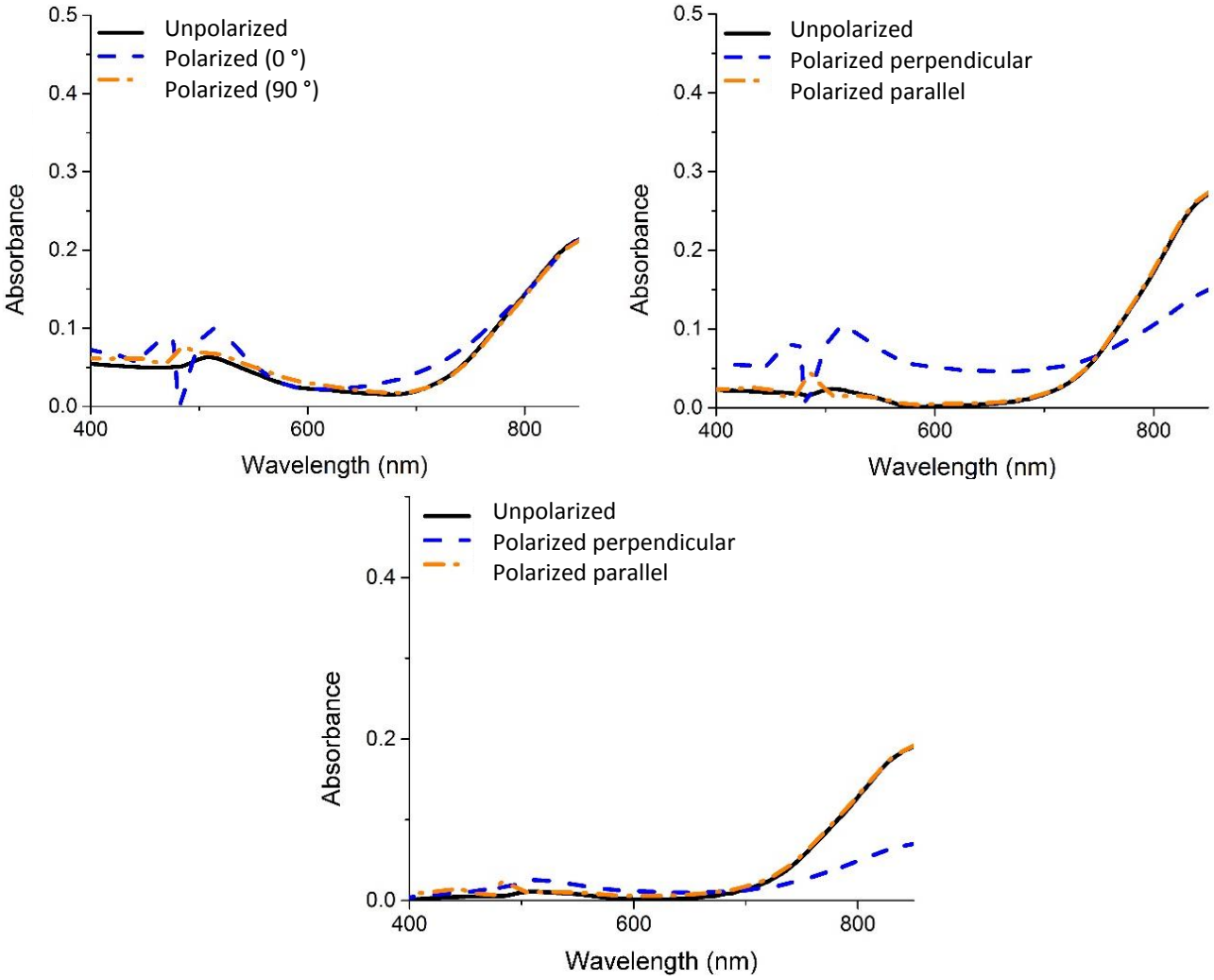

Figure 3.13 UV-Vis spectra of films made with DVD-R templates: Before stretching (top, left), after stretching in the direction of the tracks (top, right), and after stretching perpendicular to the tracks (bottom). The solid, black lines (———) are spectra obtained without polarization. The dashed, blue trace (- - -) is for light polarized in the 0° direction for the unstretched film and for light polarized perpendicular to the stretch direction in both of the stretched samples. The dash-dot, orange line (- · -) is the spectra of light polarized in the 90° direction for the sample before stretching and the spectra obtained with light polarized in the direction of stretching in the stretched samples. These were taken using the Perkin-Elmer Lambda 900 UV-Vis-NIR spectrophotometer.

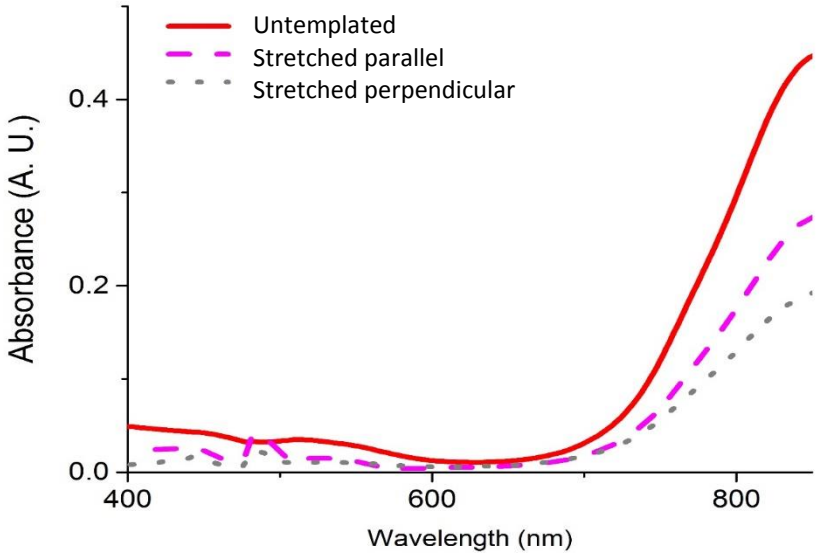

Figure 3.14 UV-Vis spectra of stretched polymer-nanoparticle composite films all polarized in the direction of the stretching. The red, solid trace (———) is the sample made without a template, the purple, dashed trace (- - -) is from the sample using a DVD-template and stretched along the tracks, and the gray, dotted line (- - -) is from the sample using a DVD-template and stretched perpendicular to the tracks. These were taken using the Perkin-Elmer Lambda 900 UV-Vis-NIR spectrophotometer.

3.5 References

[1] Gole, A., C. J. Murphy "Polyelectrolyte-Coated Gold Nanorods: Synthesis, Characterization and Immobilization" *Chemistry of Materials* **2005**, *17*, 1325-1330.

[2] Decher, G. "Fuzzy Nanoassemblies: Toward Layered Polymeric Multicomposites" *Science* **1997**, *277*, 1232-1237.

[3] Caruso, F., H. Lichtenfeld, E. Donath, H. Mohwald "Investigation of Electrostatic Interactions in Polyelectrolyte Multilayer Films: Binding of Anionic Fluorescent Probes to Layers Assembled onto Colloids" *Macromolecules* **1999**, *32*, 2317-2328.

[4] Caruso, F. "Nanoengineering of Particle Surfaces" *Advanced Materials* **2001**, *13*, 11-22.

[5] van der Zande, B. M. I., G. J. M. Koper, H. N. W. Lekkerkerker "Alignment of Rod-Shaped Gold Particles by Electric Fields" *Journal of Physical Chemistry B* **1999**, *103*, 5754-5760.

[6] Hammond, M. R., H. Dietsch, O. Pravaz, and P. Schurtenberger "Mutual Alignment of Block Copolymer-Magnetic Nanoparticle Composites in a Magnetic Field" *Macromolecules* **2010**, *43* 8340-8343.

[7] Mauter, M. S., M. Elimelech, C. O. Osuji "Nanocomposites of Vertically Aligned Single-Walled Carbon Nanotubes by Magnetic Alignment and Polymerization of a Lyotropic Precursor" *ACS Nano* **2010**, *4* (11), 6651-6658.

[8] Ryan, K. M., A. Mastroianni, K. A. Stancil, H. Liu, and A. P. Alivisatos "Electric-Field-Assisted Assembly of Perpendicularly Oriented Nanorod Superlattices" *Nano Letters* **2006**, *6* (7) 1479-1482.

[9] Shen, Y. R. "Surface Properties Probed by Second-Harmonic and Sum-Frequency Generation" *Nature* **1989**, *337*, 519-525.

[10] Van Cott, K. E., M. Guzy, P. Neyman, C. Brands, J. R. Heflin, H. W. Gibson, R. M. Davis "Layer-By-Layer Deposition and Ordering of Low-Molecular-Weight Dye Molecules for Second-Order Nonlinear Optics" *Angewandte Chemie* **2002**, *41*, 3236-3238.

[11] Chen, K., C. Durak, J. R. Heflin, H. D. Robinson "Plasmon-Enhanced Second-Harmonic Generation from Ionic Self-Assembled Multilayer Films" *Nano Letters* **2007**, *7*, 254-258.

[12] Heflin, J. R., M. T. Guzy, P. J. Neyman, K. J. Gaskins, C. Brands, Z. Wang, H. W. Gibson, R. M. Davis, K. E. Van Cott "Efficient, Thermally Stable, Second Order

Nonlinear Optical Response in Organic Hybrid Covalent/Ionic Self-Assembled Films" *Langmuir* **2006**, *22*, 5723-5727.

[13] Garg, A., R. M. Davis, C. Durak, J. R. Heflin, H. W. Gibson "Polar Orientation of a Pendant Anionic Chromophore in Thick Layer-by-Layer Self-Assembled Polymeric Films" *Journal of Applied Physics* **2008**, *104*, 53116.

[14] Chen, K., C. Druak, A. Garg, C. Brands, R. M. Davis, J. R. Heflin, H. D. Robinson "Interface Effects in Plasmon-Enhanched Second-Harmonic Generation From Self-Assembled Multilayer Films" *Journal of the Optical Society of America B* **2010**, *27*, 92-98.

[15] Fan, W., S. Zhang, N.-C. Panoiu, A. Abdenour, S. Krishna, R. M. Osgood, Jr., K. J. Malloy, S. R. J. Brueck "Second Harmonic Generation from a Nanopatterned Isotropic Nonlinear Material" *Nano Letters* **2006**, *6*, 1027-1030.

[16] Ishifuji, M., M. Mitsuishi, T. Miyashita "Bottom-up Design of Hybrid Polymer Nanoassemblies Elucidates Plasmon-Enhanced Second Harmonic Generation from Nonlinear Optical Dyes" *Journal of the American Chemical Society* **2009**, *131*, 4418-4424.

[17] van der Zande, B. M. I., L. Pages, R. A. M. Hikmet, and A. van Blaaderen "Optical Properties of Aligned Rod-Shaped gold Particles Dispersed in Poly(vinyl alcohol) Films" *Journal of Physical Chemistry B* **1999**, *103*, 5761-5767.

[18] Murphy, C. J. and C. J. Orendorff "Alignment of Gold Nanorods in Polymer Composites and on Polymer Surfaces" *Advanced Materials* **2005**, *17*, 2173-2177.

[19] Maier, S. A., M. L. Brongersma, P. G. Kik, S. Meltzer, A. A. G. Requicha, and H. A. Atwater "Plasmonics--A Route to Nanoscale Optical Devices" *Advanced Materials* **2001**, *13*, 1501-1505.

[20] Haes, A. J., R. P. Van Duyne "A Nanoscale Optical Biosensor: Sensitivity and Selectivity of an Approach on the Localized Surface Plasmon Resonance Spectroscopy of Triangular Silver Nanoparticles" *Journal of the American Chemical Society* **2002**, *124*, 10596-10604.

[21] Kumar, J., K. G. Thomas "Surface-Enhanced Raman Spectroscopy: Investigations at the Nanorod Edges and Dimer Junctions" *Journal of Physical Chemistry Letters* **2011**, *2*, 610-615.

[22] Joseph, S. T. S., B. I. Ipe, P. Pramod, K. G. Thomas "Gold Nanorods to Nanochains: Mechanistic Investigations on Their Longitudinal Assembly Using α,ω-Alkanedithiols Interplasmon Coupling" *Journal of Physical Chemistry B* **2006**, *110*, 150-157.

[23] Kumar, J., X. Wei, S. Barrow, A. M. Funston, K. G. Thomas, P. Mulvaney ”Surface Plasmon Coupling in End-to-End Linked Gold Nanorod Dimers and Trimers” *Physical Chemistry Chemical Physics* **2013**, *15*, 4258-4264.

[24] Liu, K., C. Resetco, E. Kumacheva “Salt-Mediated Kinetics of the Self-Assembly of Gold Nanorods End-Tethered with Polymer Ligands” *Nanoscale* **2012**, *4*, 6574-6580.

[25] Ghezelbash, A., B. Koo, B. A. Korgel “Self-Assembled Stripe Patterns of CdS Nanorods” *Nano Letters* **2006**, *6*, 1832-1836.

[26] Gupta, S., Q. Zhang, T. Emrick, T. P. Russell “’Self-Coralling’ Nanorods under an Applied electric Field” *Nano Letters* **2006**, *6*, 2066-2069.

[27] Sonnichsen, C., A. P. Alivisatos “Gold Nanorods as Novel Nanobelaching Plasmon-Based Orientation Sensors for Polarized Single-Particle Microscopy” *Nano Letters* **2005**, *5*, 301-304.

CHAPTER 4

CONCLUSIONS AND FUTURE WORK

Simplistic methods for creating gold nanorods of desired size and surface chemistry were explored and used in multiple applications. Polymer-nanoparticle composites were constructed and tested for dispersity and alignment. Shear alignment using a DVD as a template was shown to be a quick and cheap method to create arrays of gold nanoparticles.

AFM studies are currently being completed at this time and will allow for elucidation of effectiveness of templated alignment of gold nanorods using DVDs. The effectiveness will be determined using statistical analysis of average degree of rotation from a straight line. The side-to-side and end-to-end distances between individual gold nanorods must also be determined.

Determination of the best template size and concentration of gold nanorods within a nanorod-polymer composite can be done systematically with gratings of various widths and spacings. Using a shape memory polymer is the ultimate goal of the work as it would allow for true on-and-off capabilities of devices made using shear alignment.